8-2015

An Optimization Approach for Energy Efficient Coordination Control of Vehicles in Merging Highways

Jackeline Rios-Torres
Clemson University

AN OPTIMIZATION APPROACH FOR ENERGY EFFICIENT COORDINATION CONTROL OF VEHICLES IN MERGING HIGHWAYS

A Dissertation
Presented to
the Graduate School of
Clemson University

In Partial Fulfillment
of the Requirements for the Degree
Doctor of Philosophy
Automotive Engineering

---

by
Jackeline Rios-Torres
August 2015

Accepted by:
Dr. Pierluigi Pisu, Committee Chair
Dr. Beshah Ayalew
Dr. Robert Prucka
Dr. Ardalan Vahidi

ABSTRACT

Environmental concerns along with stronger governmental regulations regarding automotive fuel-economy and greenhouse-gas emissions are contributing to the push for development of more sustainable transportation technologies. Furthermore, the widespread use of the automobile gives rise to other issues such as traffic congestion and increasing traffic accidents. Consequently, two main goals of new technologies are the reduction of vehicle fuel consumption and emissions and the reduction of traffic congestion. While an extensive list of published work addresses the problem of fuel consumption reduction by optimizing the vehicle powertrain operations, particularly in the case of hybrid electric vehicles (HEV), approaches like eco-driving and traffic coordination have been studied more recently as alternative methods that can, in addition, address the problem of traffic congestion and traffic accidents reduction.

This dissertation builds on some of those approaches, with particular emphasis on autonomous vehicle coordination control. In this direction, the objective is to derive an optimization approach for energy efficient and safe coordination control of vehicles in merging highways. Most of the current optimization-based centralized approaches to this problem are solved numerically, at the expense of a high computational load which limits their potential for real-time implementation. In addition, closed-form solutions, which are desired to facilitate traffic analysis and the development of approaches to address interconnected merging/intersection points and achieve further traffic improvements at the road-network level, are very limited in the literature. In this dissertation, through the application of the Pontryagin's minimum principle, a closed-form solution is obtained

which allows the implementation of a real-time centralized optimal control for fleets of vehicles. The results of applying the proposed framework show that the system can reduce the fuel consumption by up to 50% and the travel time by an average of 6.9% with respect to a scenario with not coordination strategy. By integrating the traffic coordination scheme with in-vehicle energy management, a two level optimization system is achieved which allows assessing the benefits of integrating hybrid electric vehicles into the road network.

Regarding in-vehicle energy optimization, four methods are developed to improve the tuning process of the equivalent consumption optimization strategy (ECMS). First, two model predictive control (MPC)-based strategies are implemented and the results show improvements in the efficiency obtained with the standard ECMS implementation. On the other hand, the research efforts focus in performing analysis of the engine and electric motor operating points which can lead to the optimal tuning of the ECMS with reduced iterations. Two approaches are evaluated and even though the results in fuel economy are slightly worse than those for the standard ECMS, they show potential to significantly reduce the tuning time of the ECMS. Additionally, the benefits of having less aggressive driving profiles on different powertrain technologies such as conventional, plug-in hybrid and electric vehicles are studied.

DEDICATION

To God, my guide and my strength

To my parents, Aurora and Jaime, an example of tenacity and hard work

To my beloved husband, Gabriel, who has always believed in me and has been my greatest support and motivation in this journey

And, to my adorable sisters and niece: Diana, Julieth, Natalia and Gabriela, so that they always remember that with discipline and some sacrifice we can overcome the difficulties and even enjoy life

ACKNOWLEDGMENTS

This dissertation is the product of the teachings, guidance and encouragement of my mentors, professors and peers, along with love and support of my family and friends. As financial support is important to make research possible, I gratefully acknowledge the support of the Laboratory Directed Research and Development program of the Oak Ridge National Laboratory, the NSF and the DOE GATE Center program at CUICAR.

I want to express my sincere gratitude to my ORNL mentor, Dr. Andreas Malikopoulos, for his time and the priceless and kind advices, support and instruction to conclude this phase of my academic life. I also express gratitude toward my academic advisor at CUICAR, Dr. Pierluigi Pisu, for his teachings and time. I would like to give special thanks to Dr. Imtiaz Haque, Dr. Laine Mears and Dr. Zoran Filipi for their kind advises and encouragement; to Dr. Joachim Taiber and to my ORNL supervisor, Dr. David Smith for their support. I also acknowledge the contribution of my committee members and professors at CUICAR to my professional development.

Special thanks also to my family and my lovely husband for his patience and support, to my friends Julie, Pablo y Andrea for their unconditional friendship and support as well as their sense of humor, to Xueyu, Papeeha, Zoleikha, Sara and Satadru for the time shared to learn, do homework and have some enjoyment in this journey; to Perry, John and Kavit, exemplary friends. And last but not least, thanks to all the staff members at CUICAR for their kindness and willingness to help when needed. Despite the difficulties along the road, you all have contributed to make this a fulfilling experience!

TABLE OF CONTENTS

Page

Table of Contents (Continued)

Page

LIST OF TABLES

Table Page

LIST OF FIGURES

Figure Page

List of Figures (Continued)

Figure Page

List of Figures (Continued)

Figure Page

CHAPTER ONE

1. INTRODUCTION

1.1 Objective

The primary objective of this dissertation is to investigate strategies with potential to achieve energy consumption reduction in the transportation sector. In particular, this dissertation proposes the use of optimal control theory to develop an optimization framework for fluent and *energy-efficient* coordination of vehicles in merging highways or intersections which has potential for real-time implementation. The dissertation focused in finding answers to four fundamental research questions:

1. What are the effects of having smoother driving on the vehicle's energy consumption?
2. How to control the traffic to allow smooth and continuous driving on merging highways to optimize the energy use of the transportation network?
3. What is the appropriate optimization control method to obtain a closed-form solution with potential for real-time implementation?
4. What will be the impact of integrating hybrid electric vehicles into the merging control system?

1.2 Motivation

According to the US Department of Transportation, the vehicle miles traveled have increased annually by an average of 1.7% since 1990 [1]. This is just one of the facts raising environmental concerns and uncertainty about the sufficiency of oil reserves.

Furthermore, the widespread use of the automobile generates other issues such as increased traffic accidents and traffic congestion. Intersections and merging roadways or on-ramps can be considered one of the primary sources of bottlenecks further contributing to traffic congestion, which worsens at peak hours, originating a stop-and-go operation of vehicles which account for additional fuel consumption.

In the United States, on average, 5.5 billion hours are wasted each year due to vehicular congestion, which translates to about $121 billion [1]. Moreover, the reduced speed imposed by traffic congestion can produce driver discomfort and distraction. The limitation in mobility may also generate driver frustration, irritation, and stress, which may encourage more aggressive driving behavior and further slow the process of recovering free traffic flow [2].

Safety and environmental issues are also attributed to the transportation industry. In 2012, 2.2 million nonfatal injuries and 35,000 deaths were reported, and around 1.7 billion metric tons of CO_2 were released to the environment [1]. Factors such as these, along with stronger governmental regulations, are contributing to the push for development of more sustainable transportation technologies. Two main goals of the new technologies are the reduction of vehicle fuel consumption and emissions and the improvement (reduction) of traffic congestion. While an extensive list of published work attempts to address the problem of fuel consumption reduction by optimizing the vehicle powertrain operation, particularly in the case of hybrid electric vehicles (HEV), more recently, approaches like eco-driving and autonomous vehicle coordination are also being

explored as alternative methods which can, in addition, address the problem of traffic congestion.

Several approaches have been proposed for the as a measure to improve the traffic flow. While heuristic methods are the most common choice with high potential for real time implementation, their lack of optimality and sometimes their low capacity to adapt to changing traffic conditions become their main drawbacks. On the other hand, depending on how they are formulated, optimization-based approaches which can derive global optimal solutions can be complex and can only be solved numerically at the expense of high computational loads, putting at risk its potential for real time implementation.

This dissertation encompasses the improvement of the overall traffic efficiency on a portion of two convergent roads while addressing the reduction of the vehicles' energy consumption. Consequently, an optimization approach for the vehicle coordination control at merging highways is proposed, which can also be used for the in-vehicle energy optimization control for hybrid electric vehicles (HEV). In this direction, and in an effort to exploit the potential online implementation of the ECMS, I explored two paths to improve the tuning process of this strategy: 1) the use of model predictive control and, 2) the analysis of the engine and motor operating points.

1.3 Research Contribution

After a thorough literature review, the following are identified as research opportunities in autonomous traffic coordination at intersections and merging roads:

- There is a limited amount of approaches which attempt to generate a closed-form solution to the problem of automated intersection control which can adapt to different traffic conditions. Having a closed-form solution for a single intersection or merging point would be helpful to expand the problem to interconnected points and facilitate further traffic analysis and improvement at the road network level.
- Although optimization-based centralized approaches can lead to global optimal solutions, depending on the way the optimization problem is formulated, it could only be solved numerically at the expense of a high computational load which limits its potential for real-time implementation. While these approaches can still be very helpful to assess the performance of decentralized solutions and the design of eco-driving systems, this becomes a major drawback for their practical implementation.
- No attempts have been found to study the effects of introducing Hybrid Electric Vehicles into the traffic coordination system.

In summary, and to the best of my knowledge, not centralized, real-time, closed-form, optimal solutions to the problem of vehicle merging coordination are found on the literature. Therefore, the main contribution of this dissertation is the development of an optimization framework to obtain an analytical closed-form solution to the problem of centralized vehicle coordination control which addresses energy efficiency and collision avoidance and, has potential for real-time implementation.

The specific contributions in this direction are:

1. Derivation of an energy efficient, real-time implementable, closed-loop analytical solution to the problem of autonomous merging control.

2. Implementation of a centralized real-time vehicle coordination algorithm based on optimal control theory

3. Development of a benchmark system to assess the performance of decentralized solutions and the design of eco-driving assistance systems, as well as to aid in the implementation of in-vehicle energy management strategies for hybrid electric vehicles. Furthermore, having a detailed description of the dynamics of individuals merging and/or intersection points is important to conduct studies at the traffic network level. Hence, the outcomes of this research work could contribute to advances in traffic transportation and be an early step to achieve additional understanding of the interactions between entities in a highly complex system, as a traffic network, which could be used in the framework of complex systems theory for modeling and/or optimization of the transportation network.

1.3.1 Additional Contributions

A literature review in Energy Management for Hybrid Electric Vehicles allowed me to also identify that, even though the Equivalent Consumption Optimization Strategy (ECMS) is considered as one of the possibilities to overcome the computational burden of the global optimization-based approaches and achieve real-time optimal control, finding the optimal value of its equivalence coefficient is its main drawback because the requirement of accurate prediction of the future driving profile, i.e., finding its optimal

value becomes a global optimization problem too. Hence, it is desired to find a strategy to achieve its online tuning. While some efforts have been made in the past to address this issue, there is still room to achieve efficient tuning of this strategy.

In this direction, the contributions of this dissertation are:

1. Development of two model predictive control (MPC)-based strategies to improve the efficiency of the standard implementation of the equivalent consumption minimization strategy (ECMS).

2. Implementation of two numerical solutions, for the tuning process of the ECMS, based on statistical analysis of the powertrain operating points which allow for reduced tuning iterations. Furthermore, one of the solution has potential to lead to the derivation of an analytical solution to the ECMS tuning problem.

1.4 Broader Impacts

Accidents due to the transportation sector result in about 35,000 fatalities and 2.2 million injuries per year. Thus, decreasing the number of fatalities and injuries caused by traffic accidents is a critical need to, not only achieve a better quality of life in our society, but also to reduce wasted time and have a stronger economic sector. Likewise, reducing the fuel consumption and dependence of the nation of foreign oil and ameliorate the environmental burden are currently on the top priorities of the United States.

This research has the potential to help achieving a safer and more efficient transportation system, to improve the economic sector and to reduce the time wasted due to traffic. The proposed system aims at contributing with a safe and time-energy efficient

coordination of vehicles which could lead to significant reduction in deaths and injuries due to accidents in the transportation sector as well as time and energy waste.

Moreover, thinking on the proposed centralized system as a way to help advancing the development and massive use of autonomous vehicles, indirect broader impacts in the future are related to the possibility to provide mobility and independence to the elderly and disabled people as well as increment the productivity of the citizens by freeing their travel time to accomplish different activities.

1.5 Research Scope

The research is limited to the coordination of conventional engine-powered vehicles at merging highways and the analysis of the impacts of integrating hybrid electric vehicles into the coordination system. It is assumed the vehicles on the road network are autonomously driven or there is a driver following the instructions given by the centralized controller with a 100% accuracy. The analysis of the uncertainty produced by drivers who do not follow the given instructions is considered as an extension of the research but not included as a part of the dissertation.

As an attempt to achieve real-time optimization for additional energy consumption reduction in the case of hybrid electric vehicles, alternative approaches for the tuning of the ECMS are explored and numerical solutions are proposed, leaving the possibility to find an analytical solution as a future work.

1.6 Dissertation Organization

This dissertation work explores different methods for the optimization of the vehicle's energy utilization such as in-vehicle energy management, eco-driving and particularly, traffic control at merging/intersecting roads. Consequently, chapter two present a detailed overview of the main approaches find in the literature about these three areas. Chapter three investigates strategies to achieve more efficient tuning strategies for the equivalent consumption minimization strategy (ECMS). The effects of having optimized/smoother driving profiles are explored in chapter four. Chapter five is concerned with the formulation and derivation of the optimal control solution for the traffic intersection coordination problem. Finally, the conclusions and future work are discussed in chapter six.

1.7 Dissemination of results

1.7.1 Journal

1) **J. Rios-Torres**, A. A. Malikopoulos, P. Pisu. Optimal Control of Vehicle Coordination for Efficient Traffic Flow at Merging Roads. **Submitted for evaluation** to IEEE Transactions in Intelligent Transportation Systems.

2) **J. Rios-Torres,** A. A. Malikopoulos, P. Pisu. A Survey on Driver Feedback Systems and Coordination of Connected and Automated Vehicles. **Submitted for evaluation** to IEEE Transactions in Intelligent Transportation Systems.

3) **Rios-Torres**, J., Sauras-Perez, P., Alfaro, R., Taiber, J. et al., "Eco-Driving System for Energy Efficient Driving of an Electric Bus," **SAE International Journal of Passenger Cars** – Electron. Electr. Syst. 8(1):2015, doi:10.4271/2015-01-0158.

4) Y. He., **J. Rios**, M.Chowdhury, P. Pisu. Forward Power-Train Energy Management Modeling for Assessing Benefits of Integrating Predictive Traffic Data into Plug-in-Hybrid Electric Vehicles**. Transportation Research Part D: Transport and Environment,** Volume 17, Issue 1, January 2012.

5) A. Sciaretta, L. Serrao, P.C. Dewangan, P. Tona, E.N.D. Bergshoeff, C. Bordons, L. Charmpa, Ph. Elbert, L. Eriksson, T. Hofman, M. Hubacher, P. Isenegger, F. Lacandia, A. Laveau, H. Li, D. Marcos, T. Nuesch, S. Onori, P. Pisu, **J. Rios**, E. Silvas, M. Sivertsson, L. Tribioli, A.-J. van der Hoeven, and M. Wu, "A Controller Benchmark on the Supervisory Control of a Plug-in Hybrid Electric Vehicle," **Control Engineering Practice**, Jan 2014.

1.7.2 Conference

6) **J. Rios-Torres**, A. A. Malikopoulos, P. Pisu. Online Optimal Control of Connected Vehicles for Efficient Traffic Flow at Merging Roads. **Accepted for presentation** at the 2015 IEEE 18th International Conference on Intelligent Transportation Systems.

7) **J. Rios-Torres**, P. Pisu. "An alternative approach for the equivalent consumption minimization strategy- ECMS". **In review**

8) **Rios J.**, Sauras-Perez, P., Gil, A., Lorico, A. et al., "Battery Electric Bus Simulator - A Tool for Energy Consumption Analysis," **SAE Technical Paper** 2014-01-2435, 2014, doi:10.4271/2014-01-2435.

9) **J. Rios**, P. Pisu. 2013, "A Comparative Analysis of Optimization Strategies for a Power-Split Powertrain Hybrid Electric Vehicle. **Proceedings of the FISITA 2012 World Automotive Congress**,"Springer Berlin Heidelberg, pp. 541-550.

CHAPTER TWO

2 STATE OF THE ART

2.1 Energy management for Hybrid Electric Vehicles

Stronger governmental regulations regarding automotive fuel-economy and greenhouse-gas emissions along with environmental concerns, are critical factors which are fostering new challenges for the automotive industry [1], [3]. In this context, fuel economy improvement and emissions reduction are two essential issues which increase the momentum of Hybrid Electric Vehicles (HEV's) as alternatives to address them.

In addition to an internal combustion engine (ICE), the HEV powertrain contains one or more electric machines (EM) and one or more electrical energy storage systems (EESS), commonly batteries. The higher efficiency of the electric machine and the possibility to shut down the engine while idling, favors the vehicle's efficiency and the reduction of the emissions. At the same time, the new components increase the degrees of freedom of the system adding more complexity and making more challenging the implementation of an energy control strategy to optimize the fuel consumption,

The main goal of the energy control strategy is to determine the optimal power distribution among the powertrain devices, in such a way that the fuel consumption is minimized and, the driver's power demand, the drivability and the system constraints are satisfied. Several control strategies have been proposed in the past and, they can be broadly classified into two groups: rule-based and optimization-based strategies [4], [5], [6].

The rule-based control is achieved by defining a set of heuristic rules according to the driving conditions [7], [8], [9], [10]. However, due to the dynamic characteristic of the powertrain components, they do not guarantee optimality and strongly depend on the powertrain configuration.

The optimization-based strategies can be sub-divided into global optimization and local optimization strategies [4], [5], [11]. The global optimization is a non-causal approach, i.e. it requires accurate knowledge of the future driving profile, which aims to reduce the overall fuel consumption along the trip. Dynamic Programing (DP) is a commonly used technique to solve the global optimization problem [12]–[14]. Although the results guarantee optimality, it is a computationally expensive technique, a drawback limiting its capability for real-time implementation.

On the other hand, it is possible to find a suboptimal solution by converting the global optimization problem into a local one. For this case, in addition to the chemical energy of the fuel, the electrical energy utilized should be included into the cost function in order to guarantee a near to optimal solution. Two main approaches can be identified: the Pontryagin's minimum principle [15]–[17] and the equivalent consumption minimization strategy (ECMS) [18]–[20], [21].

The ECMS differs from the Pontryagin's minimum principle in that it assumes the equivalent factor to be constant along the driving cycle [22]. In order to obtain close to optimal results, the ECMS requires a tuning process for each particular driving profile to find the optimal value of the equivalent factor [20], [22]–[24]. This tuning process can then be formulated as a global optimization problem, a formulation that restricts the

potential for online implementation of the ECMS and prevents a more extensive and practical use of this approach. Therefore, it is essential to find fast and efficient tuning methods. In this direction, some authors have attempted to adaptively adjust the equivalent factor for a particular driving profile [9], [25], [26]. In the proposed strategies the *s* coefficient is updated every T seconds using the past value(s) of the coefficient as well as the deviation of the battery state of charge from the desired reference.

2.2 Eco-driving

Eco-driving systems (Fig. 1) guide drivers to achieve a more efficient driving style. This goal is commonly accomplished by using information from fuel-efficient driving profiles that are obtained through the use of heuristic rules or optimization routines. Such information can be released to the driver online or offline. This section summarizes the main eco-driving approaches described in the literature to date.

Fig. 1. Driver information and feedback systems

2.2.1 Conventional Vehicles

Conventional vehicles are powered by the chemical energy of fuel and their fuel efficiency is very sensitive to the time spent in idling and stop-and-go patterns. Consequently, there have been research efforts to integrate some degree of traffic information into eco-driving systems to avoid their excessive transient operation. The main eco-driving approaches can be classified as optimization-based and heuristic rules-based.

Optimization-Based Approaches: In [27], [28] the problem of finding optimal trajectories by indirect fuel consumption optimization is addressed. In [27], Asadi et al. formulated the problem of minimizing velocity transients and trip time, predicting traffic using a feed-forward traffic estimator based on the gas-kinetic model and using it as a constraint for the optimization problem. Dynamic programming (DP) is used that allows achieving up to a 21% fuel economy improvement. The authors emphasized the importance of prediction accuracy in achieving the potential improvements. Traffic light schedules and timing information were used by Asadi and Vahidi [28] to find a velocity trajectory that allows crossing a traffic light during the green phase without stopping, whenever possible. It is assumed the vehicle is equipped with short range radar, which is used to guarantee the vehicle keeps a safe distance from a preceding vehicle. This way, the problem is solved on two levels: first, heuristic rules are used to calculate the reference velocity for timely arrival at green lights; second, an optimization problem to minimize the speed tracking error and the braking force is solved by model predictive

control (MPC). The Powertrain Systems Analysis Toolkit (PSAT) and Simulink were used to estimate the fuel consumption, which was improved by 47% with the proposed system. In this work, deterministic traffic light timing was assumed. To have more realistic results, the authors propose using information from synchronized or traffic-actuated lights in future work.

Kamal et al. proposed in [29], and [30] to optimize the fuel economy on a host vehicle, including some dynamics from the surrounding vehicles, and presented some traffic network analysis. In [29] the multi-objective optimization target is to minimize four weighted terms: fuel economy, acceleration, deviation from an imposed speed limit, and deviation from the desired gap distance from the preceding vehicle. The fuel economy is estimated from an engine map and the MPC problem is solved by using computation and the generalized minimum residual (C/GMRES) method. They analyzed the effects of using the proposed system on a road section with intersections controlled by traffic lights using results from a simulation in the traffic simulator AIMSUN [31]. The reported fuel consumption reduction is 9.24%. In [30], the authors proposed to optimize the velocity profile by minimizing three terms: the cruising fuel consumption (assuming the vehicle operates at steady state), the acceleration force due to road grade, and the tracking speed error (with respect to the driver-desired velocity). Each term is multiplied by a weighting term whose values are tuned through observation. Fuel consumption is estimated by using a polynomial function. The optimization problem is solved by using the C/GMRES method, showing improvements of up to 10% in fuel economy.

In [32], Kamal, Imura, Hayakawa, Ohata and Aihara addressed the problem of smoothing the traffic flow by controlling a host vehicle. In this case, the dynamic behavior of the following vehicle is included in the multi-objective optimization, and the dynamics of the *n* preceding vehicles is used to estimate the future speed trajectory of the preceding vehicle. The cost function includes four weighted terms: deviation error from desired velocity, host vehicle acceleration, following vehicle acceleration, and deviation error from the desired gap with the preceding vehicle. The optimal velocity model is used to model the following and preceding vehicle dynamics, and the C/GMRES method is used to compute the solution. Through numerical simulation the authors showed that the system is able to reduce the propagation of a traffic jam on uniformly distributed dense traffic. No results are reported on fuel economy or emissions reduction.

Zhang and Vahidi [33] proposed a predictive cruise control that uses probabilistic prediction of the preceding car position. The optimization problem aims at minimizing the vehicle's acceleration and the car-following error so that efficiency can be improved while safety requirements are met. The estimation of the probability distribution for the position of the preceding car is made using a Markov chain. The problem is solved with MPC, and 15.5% improvement in fuel economy is achieved.

Kerper et al. [34] used historical data to predict a short-term future velocity profile that is optimized to minimize fuel consumption. The Comprehensive Modal Emission Model (CMEM) is used to evaluate fuel and emissions, and a dynamic time warping algorithm is used for clustering. They reported 8.3% improvements in fuel economy. Mensing et al. [35] used DP to find the optimal eco-drive cycle. They

minimized the fuel consumption, which is estimated as a function of speed and velocity. According to the reported results, they found up to a 16% fuel consumption reduction.

Wollaeger et al. [36] proposed a two-step optimization process. First the fuel consumption optimization problem is solved with DP by using a small grid. Then, a finer grid is defined around the initial optimal solution to find the global optimal. Their method, known as “pseudo-dynamic programming,” uses traffic information to define the constraints of the optimization problem. Improvements up to 14.02% in fuel economy are reported. While the authors stated the method reduces the computational burden of the DP algorithm, no results are provided to quantify the reduction of the execution time.

In [37], Chen et al. included fuel consumption, relative velocity of the preceding vehicle, and acceleration in the cost function. Fuel consumption is calculated as a polynomial function of speed and acceleration. The results showed the fuel consumption rate remains lower than for the case of a simple car-following system at all instants of time.

In [38], Ma addressed the fuel consumption minimization problem to find an optimal velocity trajectory for the vehicle before arriving at a congested point and after the congestion clears up (in such a way that the vehicle has to accelerate to continue in “free traffic flow”). Using CMEM to evaluate fuel and emissions, he found a 30% fuel economy improvement. Malikopoulos and Aguilar [26]-[[40] investigated the driving factors that have a major impact on fuel consumption and developed a driver instructor system to provide feedback to the driver in real time to alter her/his driving style and make it more eco-friendly. The system is integrated with an optimization framework that

can be used to optimize a driving style with respect to these driving factors. The optimization problem considers minimization of fuel consumption subject to speed or time constraints. In their approach, they used sequential quadratic programming to solve the problem achieving improvements of up to 23.2% in fuel economy.

Cheng et al. [41] modeled the vehicle's instantaneous fuel consumption as a piece-wise polynomial function of engine speed and torque. In addition to fuel consumption, they penalize time and acceleration. The proposed system was experimentally tested resulting in up to a 20% improvement.

Mahler and Vahidi [42] introduced the probabilistic prediction of traffic-signal timing to find an optimal velocity profile that would maximize the potential of encountering traffic lights in the green phase. PSAT and Simulink are used to estimate the vehicles' fuel consumption, and the solution is found by solving a nonlinear programming problem. Fuel economy improvements of 16% are reported, and the authors emphasize the need to further analyze the effects of informed vehicles on uninformed vehicles, penetration rates, and fleet efficiency.

Heuristic Rules-Based Approaches: The works described in this section focus on the use of heuristic rules to find velocity profiles that reduced fuel consumption. Rakha and Kamalanathsharma [43] used signal phasing and timing information to compute ideal and/or feasible velocity profiles. The velocity profiles were used as inputs to estimate the required fuel consumption from the Virginia Tech microscopic or VT-micro model.

The approach presented by Munoz-Orgarero and Magaña [44] attempts to reduce the use of the brakes when the vehicle is approaching a traffic signal that requires the vehicle to stop. The authors used image recognition algorithms to detect a set of specific traffic signals, then the distance required to stop the vehicle without using the brakes is calculated and used to advise the driver when to release the accelerator pedal. The rolling resistance and road slope information are used in the speed calculation. Fuel consumption is calculated from the mass air flow sensor and the vehicle speed obtained from the OBD2 port. From the experimental results they concluded that decelerations greater than 1.5 m/s2 produce an exponential increment in fuel consumption and confirmed that smooth acceleration patterns correlate to reductions in fuel consumption.

In [45], Jiménez et al. proposed to define a set of action rules based on the information obtained after applying DP to solve the optimization problem for a variety of road segments. The fuel consumption estimation for the optimization problem is found by using a fuel consumption map. Road slope is considered in the system model. The proposed system allows real-time advice, accounting for traffic information (updates based on required travel time and remaining trip distance). Using the Quasi-Static Toolbox (QSS) in MATLAB/Simulink, they found that fuel consumption can be improved by up to 8%.

In [46], Vagg et al. used information about the time between peaks and troughs of the speed profile, the acceleration, and the relative positive acceleration, which is a function of position, speed and acceleration, to give feedback to the driver in real time.

The feedback includes gear shifting advice. Experimental testing showed the proposed system provides average fuel savings of 7.6%.

Wang et al. [47] deal with the minimization of emissions. They used an emissions map to derive a speed profile that produces minimum emissions and used it as a reference speed. The proposed multi-objective problem includes the cost of deviations from the emissions-optimal speed, the cost of deviation from a desired speed, the cost of deviating from the desired gap with the preceding vehicle, and, finally, the cost of high acceleration values. The problem is solved through DP for uniform prediction time windows. Simulations were performed for a 1 km single lane ring road for two average vehicle densities and assuming all the vehicles are equipped with the system. The results show that using the system's reduced CO2 emissions rate can reduce emissions by 3.1% in free traffic and 9.1% under moderately congested conditions.

2.2.2 Hybrid and Plug-in Hybrid Vehicles

Hybrid electric vehicles (HEVs) (Fig. 2) and plug-in HEVs (PHEVs) have attracted considerable attention due to their potential for reducing petroleum consumption and greenhouse gas (GHG) emissions. This capability is mainly attributed to the following: 1) the potential for downsizing the engine; 2) the capability of recovering energy during braking, and thus recharging the energy storage unit (e.g., battery or ultracapacitor); and 3) the ability to minimize engine operation at speeds and loads where fuel efficiency is low. In addition, hybridization of conventional powertrain systems, which typically refers to the power requirements for the electric motor or the degree of

electrification, allows elimination of near-idle engine operation, thus enabling direct fuel economy enhancement. A typical HEV consists of the fuel converter (internal combustion engine), the inverter, the battery, and the electric machines (motor and generator).

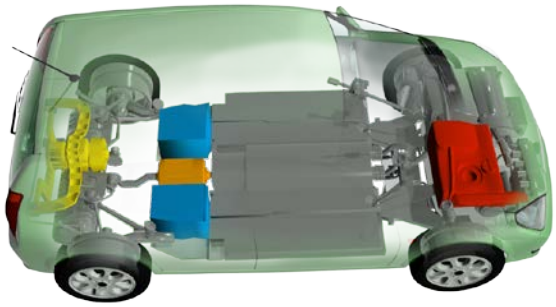

Fig. 2. HEV configuration showing the engine (red), the inverter (orange), the battery packages (blue), and the electric machines (yellow).

HEVs may be categorized, based on architecture, as one of three types: 1) parallel, 2) series, or 3) power split. In parallel HEVs, both the engine and the motor are connected to the transmission, and thus, they can power the vehicle either separately or in combination. The series HEV, in which the electric motor is the only means of providing the power demanded by the driver, is the simplest HEV configuration. Finally, the power split HEV can operate either as a parallel or a series HEV, combining the advantages of both. PHEVs are hybrid vehicles with rechargeable batteries that can be restored to full charge by connecting a plug to an external electric wall socket. A PHEV shares the characteristics of both an HEV, having an electric motor and an internal combustion engine, and an all-electric vehicle (EV), having a plug to connect to the electrical grid. This is especially appealing in situations where daily commuting is within a small

amount of miles. These vehicle architectures usually have regeneration capabilities, which allows them to be more efficient in transient operation.

Attempts to develop eco-driving systems for these HEV architectures frequently involve in-vehicle optimization. Calculating optimal deceleration patterns that maximize the energy recuperation along a route is the focus of Van Keulen et al. [48]. Using vehicle mass and geographical information to take advantage of road elevations, they predict the velocity profile for a particular route. Then they compute the required deceleration that allows the electric machine to generate at its maximum value and avoid the use of the mechanical brakes. The predicted speed profile is used later to find the optimal controls for in-vehicle energy management.

In [49] and [50], Van Keulen et al. and Vajedi et al. proposed to divide the route into segments and to define a particular optimal trajectory shape for each segment. Then nonlinear programming is used to find the parameters for each segment that minimizes fuel consumption. Improvements of up to 5% and 18.2%, respectively, are reported for each approach. Mensing et al. [51] proposed to find the optimal velocity trajectory by minimizing the fuel consumption, state-of-charge variation rate, and time. The problem is solved using DP, yielding an improvement of 10% in fuel consumption.

2.2.3 All-Electric Vehicles

EVs are powered by an electric motor and a battery. The range or maximum number of miles the vehicle can travel without recharging is an important characteristic

defining vehicle performance. The main goal of eco-driving systems for this vehicle architecture is increasing the vehicle range.

Energy consumption optimization is the focus of two studies reported in the literature recently [52], [53]. Through heuristic rules in [52] they find the feasible range that allows a vehicle to pass through traffic lights without stopping. This information is used to constrain the optimization problem, which is solved by nonlinear programming. In [53], the authors present a macroscopic steady-state analysis of an urban traffic network subject to boundary flows affected by traffic lights and variable speed limits. The cell transmission model, adapted to urban traffic, is used to model the system. In this model it is assumed that the vehicles on the road travel at an equilibrium speed. Thus, the road section is divided into homogeneous cells to represent the traffic flow. In this particular study, there are two representative cells: the congested cell and the free cell. The coauthors solve a multi-objective optimization problem to select the optimal velocity of the free cell using the instantaneous travel time, total travel time, total travel distance, and energy at the macroscopic level as the parameters of the cost function. Through the simulation of a road section with two traffic lights it was shown that the problem has a nontrivial solution.

Freuer and Reuss [54] used predictive route data and information from a radar sensor to optimize energy use by minimizing the electric powertrain losses. The optimization problem is solved online using DP for horizons of different lengths depending on the available predictive data. Experimental results show the system is able

to reduce the vehicle's energy use. A similar approach is presented by Dibb et al. [55] where the battery power is calculated as a polynomial function of speed and torque.

More recently, Rios-Torres et al. adapted and applied the optimization framework proposed by Malikopoulos and Aguilar for conventional vehicles [39], [40], to implement a driver feedback system for an electric bus [56]. In their work, the optimal problem involves the minimization of the instantaneous vehicle power consumption which is modeled as a function of the speed and acceleration. Given the dimensions of the vehicle, the grade has a non-negligible impact on the vehicle power request. Thus, it is included in the instantaneous power meta-model which was generated by using experimental data from a real battery electric bus. In addition, the authors proposed a driver feedback interface and a driver scoring method to allow the driver improving the driving skills. The authors reported improvements of up to 30.33% in power consumption.

Based on the reported review, it appears that most of the research in eco-driving to date has focused on conventional vehicles. Given the differences between internal combustion engines and electric machines, speed trajectories that are optimal for conventional vehicles are not necessarily optimal for hybrid electric or electric powertrains. Furthermore, given the different aerodynamics of light- and heavy-duty vehicles, optimal speed trajectories for them are not necessarily the same either. In addition, the following points can be emphasized.

- ✓ Most of the eco-driving approaches address the issue of finding a fuel/energy optimal speed profile for a single vehicle.

- ✓ DP is the most common approach to solve the optimization problem, limiting the possibility of real-time implementation.
- ✓ When attempting to account for traffic, traffic lights and car following have been the parameters most extensively used; minimum consideration has been given to ramps, intersections, or lane changing.
- ✓ Most of the papers predict or assume traffic information is available and use it to set constraints for the optimization problem.
- ✓ For hybrid vehicles, it is common to have a two-level optimization. Typically, in the first level there is in-vehicle optimization and in the second level, the speed profile is optimized to achieve further improvements.

It can be seen that most of the published work focuses on finding an optimal velocity profile for a single vehicle by solving similar optimization problems and adding or neglecting particular parameters. DP and MPC seem to be the preferred tools to solve the optimization problem. Thus, it is possible to conclude that currently most of the papers addressing the problem of eco-driving build upon the same basic concepts.

More recently some researchers have started exploring the effects of eco-driving systems on traffic networks and the possibilities of creating eco-driving systems for a fleet of vehicles or an entire vehicular network. Most of the research in this direction is focused on trying to find a speed trajectory that avoids collision and minimizes time. Thus, delay time is the performance metric mainly used to evaluate the effectiveness of the approaches. This new trend may lead to meaningful contributions to the sustainability

of the entire transportation infrastructure. Some common approaches reported in the literature in this area for the particular case of intersection control are detailed next.

2.3 Autonomous intersection control

Traffic lights are considered one of the most efficient ways to control the traffic through intersections and attempts are still being made in order to increase their effectiveness. Some of the more common approaches in this direction are presented by Li, Wen and Yao in [57]. However, with the appearance of V2V and V2I communication, and the increasing interest in automated vehicle technologies, the requirement of safe and efficient autonomous driving and intersection control algorithms is gaining more interest.

Vehicle coordination control, including autonomous intersection and merging control, may lead to meaningful contributions to the sustainability of the entire transportation infrastructure. In this direction, the reported approaches can be broadly classified into centralized and decentralized approaches (Fig. 3). A significant portion of them are based on the use of reservation algorithms, multiagent systems, optimization, fuzzy logic, or polling strategies. When optimization is involved in the solution the most common tools to solve it are MPC, nonlinear programming, and mixed integer linear optimization.

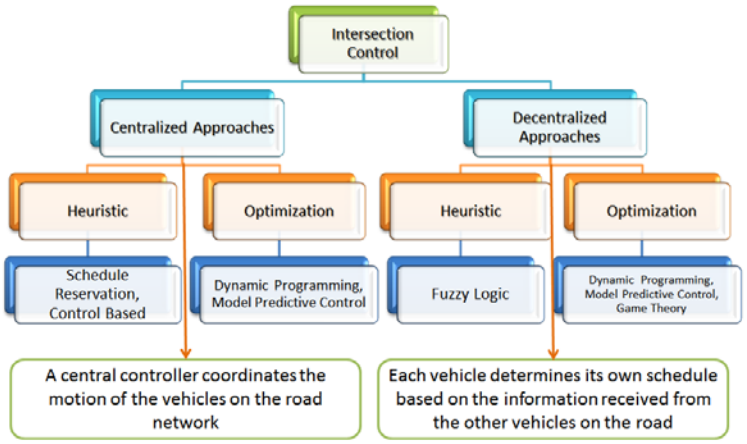

Fig. 3. Classification of autonomous intersection control approaches

Some of the first attempts to achieve a more efficient coordination of vehicles at intersections can be found back in 1977 when Pappis, and Mamdani [58] proposed the use of fuzzy logic to find more efficient switching times for the red and green cycles of a traffic light. Since then, the advances in technology has made possible the implementation of adaptive traffic lights which can adapt to the changing traffic conditions to reduce the traffic congestion[59]. However, nowadays the interest in connected and autonomous vehicles technologies is gaining momentum, which propels, among others, the development of algorithms for autonomous intersection and merging control. In this direction, back in 2008, Dresner and Stone [60] proposed a centralized system to achieve automated vehicle intersection control. After that, several approaches have been proposed to achieve safe and efficient autonomous control of the traffic through intersections and merging highways which can be broadly categorized as centralized and decentralize. Here, we categorize an approach as centralized if there is at least one task in the system that is globally decided for all vehicles by a single central

controller or coordinator. In the following subsections we formulate the intersection control problem and discuss the various approaches in each of these categories, i.e., centralized, decentralized.

2.3.1 General problem formulation

Typically, the crossing sequence on an intersection is controlled by traffic lights or stops signs which implies that, at some time, the vehicles on one road have to stop to concede the right of way to the vehicles on the other road. Fig. 4 illustrates a common intersection scenario in which it is possible to improve the traffic flow by using connected vehicle technologies, and thus minimizing the time for the vehicle spent idling. In such typical scenario, a control zone is defined as the section of the roads located inside a radius L of the intersection.

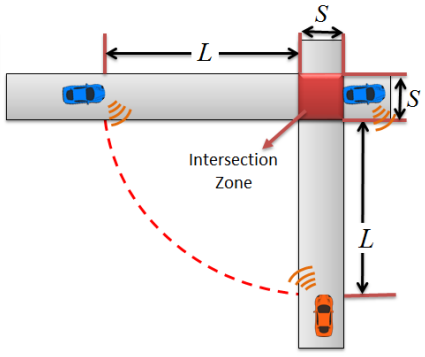

Fig. 4. Simplest intersection scenario

Based on the scenario illustrated in Fig. 4, it is assumed that the vehicles in the system are subject to a second order dynamics (1)

$$\dot{x}_{j,i} = v_{j,i}$$
$$\dot{v}_{j,i} = u_{j,i} \quad (1)$$

where $j = \{1, 2, ..., m\}, m \in \mathbb{N}$, indexes the road, $i = \{1, 2, ..., n\}, n \in \mathbb{N}$, indexes each vehicle, x is the position of each vehicle, v is its speed, and u is the control input, which is vehicle's acceleration. L is the length of the control zone and S is the length of the intersection zone. Eventually, when it is necessary to differentiate among the roads and vehicles, the subscripts p and q will be used for the road and vehicles respectively.

The general autonomous intersection control problem considers finding a control policy to coordinate the crossing sequence of the vehicles while satisfying certain constraints, i.e., avoiding collisions and minimizing travel time. It is possible to solve this problem through optimal control. Different formulations have led to different possible approaches. Some of the most common formulations in the centralized and decentralized case are discussed next.

2.3.2 Centralized Approaches

In centralized control the crossing sequence and respective crossing intervals are decided by a centralized controller while satisfying the constraints imposed by the road capacity. Some of the studies discussed in this section develop the control algorithm by implementing reservation schemes while others use an optimization framework.

2.3.2.1 Reservation Scheme

In general, in this approach there is a centralized controller or intersection manager which coordinates the reservation or crossing schedule based on the requests and information received from the vehicles located inside the communication range. The intersection is divided into cells or points which are to be assigned or reserved for only one vehicle at each instant of time to avoid collisions (Fig. 5). The main challenges in this case are associated with the heavy communication requirements and the possible occurrence of deadlocks. The communication becomes a critical issue, particularly when vehicles are required to communicate several times with the central controller until their reservation request is approved.

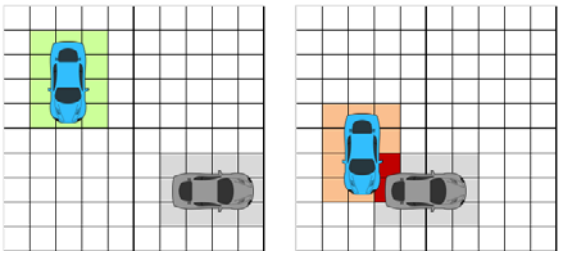

(a) (b)

Fig. 5. Cells reservation process at time t (as proposed in [57]). (a) Successful reservation. (b) Reservation request rejected due to conflict with a cell already reserved by another vehicle

In [61] Dresner and Stone proposed the use of the reservation scheme to control a single intersection of two roads with vehicles traveling with similar speed on a single direction on each road, i.e., no turns are allowed. In their approach, each vehicle is treated as a driver agent which request the reservation of the space-time cells to cross the intersection at a particular time interval which is defined from the estimated arrival time to the intersection. Once the centralized reservation system receives the request, it accepts

if there is not any conflict with the already accepted reservations, otherwise, the request is to be rejected. In case of rejection, the driver agent is required to decelerate and send a new reservation request. Note that in this case, each driver agent has autonomy to decide the best trajectory to fulfill the assigned crossing time interval. To test the efficiency of the proposed system, they measured the delay incurred by the vehicles due to the deceleration required until the reservation request is accepted. This work was later extended [60] to consider turning as well as including improvements like allowing the central controller: (1) to estimate the positions of the cars to prioritize the requests made for the vehicles which are closer to the intersection (reducing probability of deadlocks), (2) imposing the required acceleration profile inside the intersection zone and (3) send a counter offer for the arrival time and trajectory when rejecting a request. Huang et al.[62] further extended the work in [60] by (1) centralizing the computation of the vehicle trajectories to reduce the possibilities of reservation cancelation due to inability to fulfill the initially reported arrival time, (2) adopting a hierarchical processing of the reservation request which accounts for the implementation of different priority assignations and (3) in addition to the mobility metrics, the author proposed to evaluates metrics related to environmental benefits. The reservation scheme have been also explored by Au and Stone [63], De la Fortelle [64], and Zhang et al. [65].

2.3.2.2 Control Approaches

The vehicle intersection control proposed by Wuthishuwong and Traechtler [66] consists of a two-level control. In the lower level an intersection agent uses estimation of

the traffic flow to define a control policy that guarantees traffic flow stability in the intersection. In the upper level, information about traffic density for the incoming and outgoing streets is shared among the connected intersection neighborhoods to improve system throughput. At this level, the consensus algorithm is used by each intersection agent to compute desired traffic density based on the information received from connected neighbors. This desired traffic density is then used to determine desired vehicle velocity using the Greenshield model. Graph theory is used to model the network, and the results showed that the adopted average vehicle velocity allows the system to maintain stability.

Jin et al. [67] considered platoon formations for decentralized intersection control. In this work, the intersection controller communicates with the platoon leader and the leader with the followers. The platoons are defined according to the gap between adjacent vehicles and/or the size limit. Once a platoon is set, the leader calculates the time of arrival at the intersection for each vehicle and sends the information to the controller along with the request to cross the intersection. If the request is accepted, the platoon leader calculates the required vehicle trajectories to satisfy the assigned schedule and safety constraints. Simulation were performed in SUMO for a two roads intersection and the results showed up to a 23% reduction in fuel consumption and 30% reduction in travel time when compared with respect to traffic light-based and non-platoon-based approaches.

2.3.2.3 Optimal Control

Optimizing travel time. Increasing the throughput of an intersection is one desired goal to reduce traffic congestion and it can be achieved through the optimization of the travel time for all the vehicles located inside a radius L from the intersecting roads. For the scenario illustrated in Fig. 6, adopting a first come first serve (FIFO) system and allowing only one vehicle on the intersection at each instant of time, the optimization problem can be formulated as follows:

$$\min_{u} \frac{1}{2} \sum_{j=1}^{m} \sum_{i=1}^{n} \left[t_{j,i}^{out}(u) - t_{j,i}^{in}(u) \right]^2 \tag{2}$$

Subject to:

$\dot{x}_{j,i} = v_{j,i}$

$\dot{v}_{j,i} = u_{j,i}$

$\left[t_{j,i}^{out}(u) - t_{j,i}^{in}(u) \right] \geq \Delta \mathrm{T}_a$

$o < v_{j,i}(t,u) \leq v^{\max}$

$x_{j,i}(t,u) \leq x_{j,q}(t,u) + \delta$ for all $t,\ i \neq q$

$x_{j,i}(t,u) \leq x_{p,q}(t,u) + \mathrm{S}$ for all $t,\ j \neq p,\ i \neq q$

where $\Delta \mathrm{T}_a$ is the minimum allowed time (time it takes to cross at the maximum speed $v^{\max}$) and δ is the minimum safest following distance.

The approaches proposed by Li and Wang [68], Raravi et al. [69], Yan et al. [70], Zohdy et al. [71], Jin et al. [72], Wu et al. [73] and Zhu and Ukkusuri [74], focus on the formulation of an optimal control problem in which the objective function involves the travel time. The constraints, which are different in each work, are formulated with the goal of avoiding collisions. Dynamic programming (DP) is applied in [73] to solve the formulated optimization problem. As the complexity of DP increases with the addition of

lanes, the authors propose an alternative heuristic solution in which the system is modeled using Petri nets and the main goal is to minimize the sum of the lengths of the two queues. They found that platoon-based vehicular control improves traffic flow and based on this formulated rules to control the vehicle crossing sequence. A mathematical proof of this approach was presented by Wu et al. in [75].

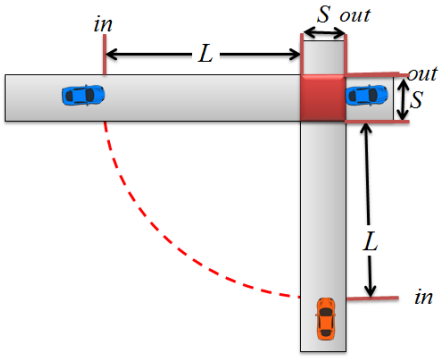

Fig. 6. Intersection collision avoidance scenario for travel time optimization

Minimizing the vehicles overlap. For the scenario illustrated in Fig. 6, assuming that the vehicles in the system follows the dynamics in (1), and that they are served on a first come first serve basis, i.e., a hierarchical sequence is established, in this approach the optimal control problem consists in minimizing the overlap of the vehicles position inside the intersection zone, i.e., the objective is to control the vehicles acceleration such that only a limited amount of vehicles are present inside the intersection at each instant of time. The total amount depend on the size of the vehicles, the length of the intersection area and the minimum safest following distance. The plot in Fig. 7 illustrates the general idea for this approach, where a is the maximum time between the time that the vehicles i and $i+1$ enter the intersection, t_i^{in} and t_{i+1}^{in} respectively, and b is the minimum time

that the vehicles i and $i+1$, exit the intersection, t_i^{out} and t_{i+1}^{out} respectively. The objective is to minimize the length of the overlapped trajectories, i.e., the integral from a to b of the length of the trajectory arc.

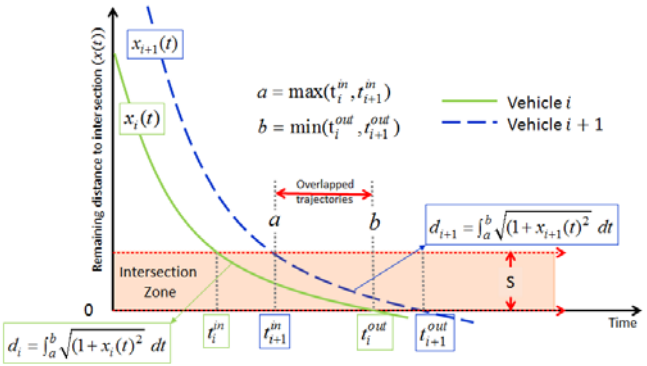

Fig. 7. Illustrative example of trajectories overlap

The general optimization problem is stated in (3). In this formulation, constraints are imposed to satisfy the minimum and maximum speed limits and acceleration as well as to keep a safe inter-vehicular distance between vehicles on the same road.

$$\min \sum_{i=1}^{n} \int_a^b \sqrt{1+x_i(t)^2}\,dt \qquad (3)$$

This approach was first proposed by Lee and Park in [76] where they considered the case of a two-roads intersection with two lanes and turning capabilities using of a phase conflict map as a part of the problem formulation. Simulation results showed that the system is not only able to reduce total travel time and delays but also able to reduce fuel consumption. This work was later extended to the case of an urban corridor [77].

Multi-objective optimization. A number of approaches have been proposed which address the problem by including more than one term into the cost function. In this case, it is common to assume that the vehicles have already been assigned a driving schedule, thus, the problem consist in minimizing the error between the actual vehicle speed and the desired speed as well as the acceleration. In this case, the optimization problem can be solved for time horizons of equal length and additional terms can be added to guarantee avoidance of collisions or achieve further time optimization. In general, this problem can be formulated as:

$$\min_{u} \sum_{k=1}^{H} \int_{t(0)+k\mathrm{T}}^{t(0)+T+k\mathrm{T}} \left[\sum_{j=1}^{m} \sum_{i=1}^{n} \left(w^{v} \left(v_{j,i}(\tau) - v^{d}(\tau) \right)^{2} + w^{u} (u(\tau))^{2} + w^{c} (f(\tau,u))^{2} \right) \right] d\tau \qquad (4)$$

where H is the total number of horizons, k denotes each horizon, T is the length of each horizon, w denotes penalty weights and $f(\tau,u)$ is any additional function, which can be used to quantify the risk of collisions in the system. The constraints vary for each formulation, but in general the most common constraints are related to the speed and acceleration limits and safest following distance or time.

This multiobjective optimization framework was used by Campos et al. [78] and Kamal et al. [79], [80]. The formulation in [78] includes speed tracking error and acceleration in the objective function to find safe trajectories while satisfying local constraints, like the avoidance of control inputs which belong to the critical set as defined in Hafner et al [81]. The set of constraints is later modified for a decentralized version of the controller in which a reservation scheme is used. Model predictive control (MPC) is used in [79], [80] to solve the multiobjective optimization problem that includes a risk

factor function to quantify the risk of collision at the intersection and constraints related to safe velocity and acceleration values.

Other optimization-based approaches. Less common approaches were presented in [82], [83] and [84] and will be briefly described. Charalampidis and Gillet [82] derived closed-form solutions to the problem of intersection control. They used a second-order kinematic model to describe the vehicle dynamics and assumed all the vehicles initially travel at a maximum speed. This way, the collision avoidance strategy consists of finding the appropriate deceleration/acceleration pattern. Once the first vehicle reaches the communication range of the intersection manager, it calculates the time required to leave the intersection and sets a reservation. Once the second vehicle is detected, it is forced to adjust speed to an optimal speed value to ensure it reaches the intersection only after the first one has already crossed it. The optimal speed is calculated by minimizing the delay due to deceleration. This approach only allows one vehicle at the intersection at a time.

Zohdy and Rakha [83] used game theory for this problem. In this application, a manager agent receives information from the vehicles in the road network and selects one of them to optimize its trajectory. At the same time, based on the available information, every vehicle agent optimizes its own trajectory. Using Monte Carlo simulations, it was shown that the proposed system is able to reduce the total delay compared to a traffic-light-controlled intersection.

The use of queueing theory to address this problem was proposed by Miculescu and Karaman [84]. In their approach, the system is modeled as a polling system with two

queues and one server. The customers (vehicles) are coordinated to cross the intersection without collisions. The polling system determines the sequence of times assigned to the vehicles on each road. Then, a coordination algorithm finds the safe trajectories for all the vehicles inside the control region using the time each vehicle should arrive to the intersection and the trajectory of the leading vehicle. Differential constraints are used to enforce safety. Simulations for light-, medium-, and heavy-load cases were performed using MATLAB. The results showed that the switching times needed to reassign the right of way from one road to another are reduced in the case of heavy loads, thus promoting platoon formations.

2.3.3 Decentralized Approaches

In decentralized control, each vehicle determines its own control policy based on the information received from the other vehicles on the road or some coordinator. One of the main challenges faced in the implementation of decentralized approaches is the possibility of having deadlocks in the solutions as a consequence of the use of local information. Various heuristic- and optimization-based decentralized control approaches have been described in the literature to date.

2.3.3.1 Decentralized Heuristic Control

Fuzzy logic. Was used by Milanes et al. [85] to design a controller that allows a fully automated vehicle to yield to an incoming vehicle in the conflicting road or to cross, if it is feasible and collision risk is not present. The fuzzy controller controls the throttle

and brake pedals of the automated vehicle and was experimentally implemented and tested on a two-road intersection in the presence of a human-controlled vehicle. In [86], Milanes et al. compare three heuristic intersection control schemes which were implemented based on: 1) Fuzzy logic, 2) Partial Motion Planner (PMP) and, 3) Heuristic static rules. The schemes were implemented in automated cars and experimental results showed they can safely interact in a cooperative environment working under a specific communication protocol. When operating in the presence of manually operated cars, the three autonomous vehicles were able to yield and stop before the intersection. The work described by Milanes et al. [85] was extended by Onieva et al. in [87]. The proposed control scheme consists of a three-layer fuzzy control system. The first layer, detects whether a turn or a straight path through the intersection is required. The second layer determines a feasible speed value to safely cross the intersection; in this layer the fuzzy algorithm is optimized by means of a genetic algorithm. The third layer determines the accelerator and brake commands required to track the speed reference given by the second layer. Simulation results showed the system was able to coordinate the vehicles without collisions.

Definition of a critical/invariant set. Based on the scenario illustrated in Fig. 8 and under the dynamics in (1), it is possible to demonstrate that the system is monotone if the following assumptions are made: 1) The control input has a unique minimum and a unique maximum, i.e. $u_{\min} \leq u_{j,i} \leq u_{\max}$, and the system (1) is non-decreasing in $u_{j,i}$, 2.) the system (1) has unique solutions, 3) only positive speeds are allowed: $v_{\min} < v_{j,i} \leq v_{\max}$,

4) $\left|\dot{v}_{j,i}\right|$ is bounded for all $v_{j,i} \in [v_{\min}, v_{\max}]$, 5) all the vehicles on the same path follow the same dynamics, i.e., $x_{j,i} = x_{j,q}$, $v_{j,i} = v_{j,q}$ for all $j \in \{1,2\}$, $i,q \in \{1,2,...,n\}$.

From the monotonicity of the system it follows that the hierarchical sequence of the vehicles is kept as long as $x_{j,i} \geq x_{j,q}$, $v_{j,i} \geq v_{j,q}$ and $u_{j,i} \geq u_{j,q}$ and this property allows the definition of a critical set. Also, according to the geometry of the intersecting roads in Fig. 8, it is possible to have rear-end collisions when the vehicles travel on the same road, or side collisions when two vehicles from different roads are entering the intersection zone at the same instant of time. The intersection zone can be represented by the interval $[x_{j,i}^{in}, x_{j,i}^{out}]$ which can be defined according to the vehicle length. Then, the critical set $CS = CS_{rear} \cup CS_{side}$ is defined as the set of all the states in which the collisions are unavoidable: $CS_{rear} = \left\{ \mathrm{x} \in \mathrm{R}^n : \exists (i,q) \,|\, \left| x_{j,i} - x_{j,q} \right| < \delta \right\}$ and , $CS_{side} = \left\{ \mathrm{x} \in \mathbb{R}^n : \exists (j,p,i,q),\, j \neq p \,|\, (x_{j,i}, x_{p,q}) \in (a_{j,i}, b_{j,i}) \cap (a_{p,q}, b_{p,q}) \right\}$. Thus, the problem consist in finding a control input $u_{j,i}$ such that $x_{j,i}(t, u_{j,i}) \notin CS$ for all $t \geq 0$, j,i.

Hafner et al. [81], [88] used the definition of the critical set in such a way that, if the current vehicle trajectories are close to the critical set, the control scheme is activated and inputs selected to lie outside the critical inputs set are applied to accelerate one vehicle and decelerate the other. Similarly, Colombo and Del Vecchio [89] proposed to find the set of control inputs that would avoid collisions, i.e., an invariant set. The problem is then translated into a scheduling problem and exact and approximated solutions are presented. In this case, the controller only modifies the trajectory of a

vehicle if it detects that the current control input is outside the set of safe control actions. These approaches does not involve optimization, and the control scheme is deactivated after the current vehicles have safely crossed the intersection.

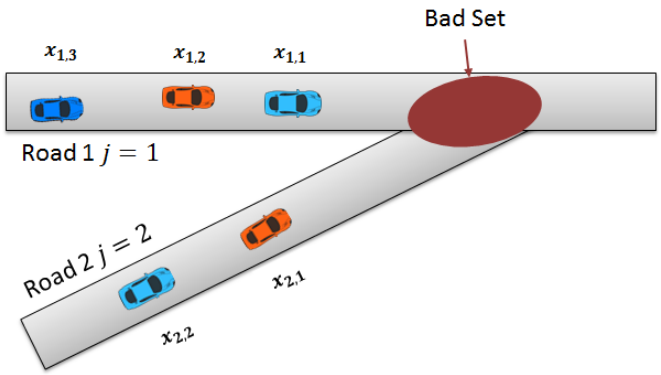

Fig. 8. Intersection collision avoidance scenario illustrating the bad set

In a similar approach, Quian et al. [90] proposed an algorithm to integrate legacy vehicles in the coordination system, i.e. manually driven vehicles with not V2V nor V2I communication capabilities. In this case, sensors located on the road will notify to the intersection controller the presence of legacy vehicles and by following predefined rules the legacy vehicles will be notified by means of a traffic light whether it is allowed or not to cross. The safety operation of the coordination algorithm was proved through simulation results, however, note that stop and go operation will still be allowed.

Other heuristic approaches. In [91], Alonso et al. proposed two conflict resolution schemes in which an autonomous vehicle could make a decision about the appropriate crossing schedule and trajectory to follow to avoid collision with other manually driven vehicles on the road. To be able to safely drive through the intersections,

the vehicles are assumed to have V2V capabilities, in particular they share information regarding their position, speed, driving direction (to recognize turning), accuracy of the position data and identification. The first scheme is based in the use of priority tables. Thus, by implementing a look up table including all the possible combinations of occupancy of the intersecting roads, a signal is defined which indicates to the vehicle whether it should continue moving or stop until the intersection is cleared. In the second scheme, each vehicle determine its own priority level and the look up table is created, so that the priority level is accounted for, to decide whether the vehicle should stop or cross. The approach was implemented and experimentally tested with three vehicles, which were able to safely interact in two different scenarios.

Wu, Zhang, Luo and Cao [92] proposed centralized and decentralized algorithms. The centralized approach uses a controller node which communicates with the vehicles to coordinate the crossing sequence. To do that, each vehicle entering the queue sends a request to the controller to put in hold the vehicles coming from conflicting lanes. The rejection or acceptance depends on the previously accepted requests and the distance left to reach the intersection. Once each vehicle exits the intersection area, it sends a message to the controller to release the vehicles on hold. In the decentralized approach, the best passing sequence is decided by wirelessly sharing the estimated arrival time among the vehicles on the queue. If any vehicle has an arrival time shorter than the current shared arrival time, it sends a message to prevent the current vehicle from crossing. This approach is a modified version of the Mutual Exclusion Problem (MUTEX) which the authors named Vehicle Mutual Exclusion for Intersections (VMEI). Additional logic is

included for simultaneous crossing of vehicles traveling on non conflicting lanes. As both schemes require fast and reliable communication, the network simulator NS-3 was used to evaluate the average queue length, average waiting time, system throughput and message cost. The two proposed approaches outperformed an adaptive traffic light approach while the centralized outperformed the distributed approach. The authors did not focus on optimizing a particular performance metric and the approach involves stop and go operation; hence, they may be missing opportunity to increase the efficiency of the system.

In an alternative path, Khoury et al. [93], proposed an algorithm which in addition to be decentralized does not rely on V2V or V2I communication, but only on the information received from local sensors. With this approach the authors attempt to achieve a low cost, secure and private (since not communication is used) solution.

2.3.3.2 Decentralized Optimal Control

Multiobjective optimization. In decentralized autonomous intersection control, multi-objective optimization solved for time horizons of equal length (T) has also been proposed. As in the centralized case, in the decentralized approaches is also common to assume that the vehicles have already been assigned a driving schedule, thus, one of the terms in the objective function attempts to minimize the error between the vehicle speed at the current time step ($v_i(l)$) and the desired speed (v^d). Minimizing the acceleration (u) and other terms that can be related to collision avoidance $f(l,u)$ is also common in

the formulations. Thus, the main difference with respect to the centralized case is the local nature of the information used to solve the optimization problem, i.e., each vehicle solves its own optimization problem based on the local information it poses and the one it receives from the vehicles located inside a particular radius from its current position. In general, the decentralized optimization problem can be formulated as:

$$\min_{u} \sum_{l=1}^{T} \left(w^{v} \left(v_i(l) - v^{d} \right)^2 + w^{u} (u_i(l))^2 + w^{c} (f_i(l, u_i))^2 \right) \tag{5}$$

The more common constraints found in the literature are related to the minimum safe distance/time gap between vehicles approaching the intersection, minimum following distance (for vehicles on the same lane) and speed and acceleration limits. The approaches presented in [94], [95], [96], [97] and [98] formulate multi-objective optimization problems.

Makarem and Gillet [96] proposed a method that assumes the vehicles are traveling at a desired vehicle speed (v^{d}) and thus, their expected time of arrival to the intersection (τ_i) can be previously calculated. Then, the control input is computed from a navigation function (ϕ_i) which attempts to minimize the error between the desired speed and the actual speed of each vehicle (v_i) while keeping a safe time gap among the vehicles attempting to cross the intersection as well as assigning smaller acceleration values to heavier vehicles compared to lighter vehicles. This last characteristic allows to assign smoother trajectories to heavier vehicles, thus reducing energy consumption. Assuming the vehicles in the system are subject to the dynamics in (1), the navigation function is mathematically formulated as in (6).

$$\phi_i = w^v (v_i - v^d)^2 + w^g \sum_{q \neq i} w_i^J (i,q) \beta_i (\tau_i, \tau_q, v_i) \quad (6)$$

Where w^v, w^g and $w_i^J = \frac{J_i}{J_q}$ are weight factors related to the speed error, time gap and vehicle inertia and β_i is a function that guarantees the vehicles will safely cross the intersection keeping a safe time difference σ to reach the intersection. A two-road intersection was simulated, and the performance of the approach was evaluated by measuring the total energy consumption and traffic flow and comparing them with those for an intersection controlled by traffic lights and those for an intersection controlled by a centralized approach. The results showed that the proposed strategy is 24% less energy efficient than the centralized approach but still more efficient than using traffic lights.

Using MPC to solve the local optimization problem has been proposed by Makarem et al. [97], Qian et al. and Kim and Kumar [98]. In the approach proposed by Makarem et al. [97] each vehicle defines its constraints by using the local information it receives from the other vehicles inside the communication range. Then, each of them solves a linear quadratic optimal control problem according to its dynamics and constraints to avoid collision. Each vehicle calculates the time required to arrive at the intersection for all the vehicles in the network so that the priority to modify the acceleration control can be given to the one which is closest to the intersection. The effectiveness of the system is confirmed through simulations. On the other hand, Qian et al. [99] proposes to solve the problem in two levels. In a high level, the vehicles are coordinated based on some predefined priority scheme. Then, a low level control will

solve a multi-objective optimization problem based on the information of its current system state and short time prediction of the states evolution of the vehicles in front.

Other optimization-based approaches. Tlig et al. [100] proposed a decentralized approach in which the vehicles are allowed to cross alternately. It is decentralized in the sense that each intersection is controlled independently. Thus, this approach still requires a centralized controller in charge of synchronizing the vehicles to achieve an alternated crossing sequence. After receiving approval to cross and the required arrival time to the intersection, each vehicle adjusts its own speed according to a previously defined ideal velocity profile which shape contains three zones: a deceleration zone, a constant speed zone, and an acceleration zone. The vehicle has to decide the optimal velocity value for the constant velocity zone and the time horizon it needs to keep such speed is computed according to the arrival time. The acceleration and deceleration rates are assume to be fixed and equal for all the vehicle. A two-road intersection was simulated and total crossing time and energy consumption were used as performance metrics. The simulation results showed the proposed approach outperformed the standard traffic light-based intersection control approach. In [101], the same authors proposed a two-level control system for interconnected intersections. In the first level, a control agent coordinates the vehicles to allow them crossing alternately and deciding their own speed. In the second level, each intersection control agent shares information with its neighboring control agents to optimize the flows inside the road network. This is achieved by optimizing the phases of each intersection so that the desired optimal speeds for each road segment can

be calculated. Simulation of a traffic network with 6 roads and 12 intersections showed that the approach allows the vehicles to cross the intersections avoiding collisions.

A significant portion of the proposed approaches on intersection control is based on the use of reservation algorithms, multiagent systems, optimization, fuzzy logic, or polling strategies. When optimization is involved in the solution the most common tools to solve it are MPC, nonlinear programming, and mixed integer linear optimization. Some authors have also attempted to use fuel/energy consumption as a performance metric; however, few attempts have been made to incorporate it directly in the trajectory optimization process. A few authors have addressed the problem of minimizing acceleration as an indirect attempt to reduce the vehicle's fuel/energy use.

A substantial amount of work has reported simulation results for a single intersection; only a few have attempted to consider interconnected intersections, which may result in a more complex problem but, could give insight of the impact on overall traffic conditions. Although the majority of work reported in the literature has demonstrated the effectiveness of the efficiency of their approaches with simulation results, very few papers have been found that attempt to generate some sort of closed-form solutions to the problem of automated intersection control.

CHAPTER THREE

3 EQUIVALENT CONSUMPTION MINIMIZATION STRATEGY (ECMS)

3.1 ECMS formulation

The main goal of an energy control strategy is to determine the optimal power distribution among the energy sources in a Hybrid Electric Vehicle (HEV), such that the fuel consumption is minimized and the driver's power demand is satisfied. It also has to meet the drivability requirements and the system constraints such as the battery state of charge (SOC) bounds and the limitation of the powertrain devices. This global optimization problem is formulated as follows:

$$\min_{\{P_{eng}(t),P_{em}(t)\}} \int_0^{T_f} \dot{m}_f(\tau)d\tau \tag{7}$$

Subject to the constraints:

$$P_{req}(t) = P_{eng}(t) + P_{em1}(t) - P_{em2}(t)$$

$$0 < SOC_{\min} \le SOC \le SOC_{\max} < 1$$

$$0 \le P_{eng}(t) \le P_{eng,\max}(t)$$

$$0 \le \omega_{eng}(t) \le \omega_{eng,\max}(t)$$

$$0 \le T_{eng}(t) \le T_{eng,\max}(t)$$

$$P_{em,\min}(t) \le P_{em}(t) \le P_{em,\max}(t)$$

$$\omega_{em,\min}(t) \le \omega_{em}(t) \le \omega_{em,\max}(t)$$

$$T_{em,\min}(t) \le T_{em}(t) \le T_{em,\max}(t)$$

Where T_f is the duration of the trip, $\dot{m}_f$ is the fuel flow rate, P is power, T is torque, ω is speed, em refers to the electric motor/generator, eng refers to the engine, p_{req} is the power request and SOC is the battery state of charge.

Dynamic Programming (DP) is commonly used to solve the global problem. However, it requires the continuous problem to be discretized, requiring a very fine grid in order to neglect the approximation error. This implies a high computational load to solve the problem which becomes a major drawback limiting its potential for real-time implementation. To overcome this drawback, the global optimization can be replaced by a local optimization problem which solution is known as the equivalent consumption minimization strategy (ECMS). The ECMS strategy is based on the assumption that a present use of the energy storage system (EESS) corresponds to a future fuel consumption that will be required to recharge it. Similarly, a present recharge of the EESS corresponds to future fuel savings since the energy will be available for future use at a lower cost [23]. For this work the EESS is a battery.

According to these assumptions, the solution of the local optimization problems is found by solving an instantaneous minimization of the equivalent fuel flow rate $\dot{m}_{f,eq}$ at each instant of time, under the same constraints as in the global approach. The instantaneous minimization problem is stated in (8), and is subject to the same constraints as in (7).

$$\min_{\{P_{eng}(t),P_{em_i}(t)\}} \dot{m}_{f,eq}(t) \quad \forall t \tag{8}$$

$$\dot{m}_{f,eq}(t) = \dot{m}_{f,\mathrm{eng}}(t) + \dot{m}_{f,eq,batt}(t)$$

Where $\dot{m}_{f,eng}$ is the engine's fuel flow rate and $\dot{m}_{f,eq,batt}$ represents an equivalent fuel flow rate related to the use of the battery power. For the general case, and assuming the equivalence factor s remains constant for the charging and discharging cases, the equivalent battery fuel flow rate is a function of the equivalence factor s, the battery power P_{batt} and the Q_{lhv} as in Eq. (9).

$$\dot{m}_{f,eq,batt} = s \cdot \frac{\beta \cdot P_{batt}}{\eta_t \cdot Q_{lhv}} \tag{9}$$

Here, s is an optimization parameter to be tuned, is related to the average powertrain efficiency in the future and its optimal value will be different for diverse driving profiles. That is, an s value that assures a close to optimal use of the battery energy for a particular driving cycle, can lead to poor use of the battery in others.

3.2 Improving the ECMS tuning through the use of MPC-based approaches[1]

For this work, the ECMS was implemented for a plug-in hybrid electric vehicle and two strategies to tune the equivalence factor, based in MPC, were developed.

3.2.1 PHEV Simulator

PHEV's powertrain architecture contains an internal combustion engine, electric motors, and two or more energy storage systems (ESS). They differ from the Hybrid Electric Vehicles in that PHEV's can be plugged-in to the electric grid to recharge the battery. The power-split powertrain for the HEV was modeled following a forward

[1] Based upon work supported by the National Science Foundation (NSF) and under Grant No. 0928744. Any opinions, findings, and conclusions or recommendations expressed in this material are those of the author(s) and do not necessarily reflect the views of the National Science Foundation

looking approach in which the simulation proceeds with the power request forward from the driver to the wheels. It includes the model of a driver to calculate the error between the velocity profile defined by the driving cycle and the current vehicle velocity, according to which the throttle and brake commands are calculated. To facilitate the on-board implementation of an energy management strategy, a simulator of the forward-looking model of PHEVs with power-split drive train was implemented in Matlab/Simulink. The main components and parameters were based on the Toyota Prius second generation PHEV (Table 1).

Table 1. Main parameters of the power-split power-train

Parameter	Symbol	Value
Vehicle mass	m	1330 kg
Aerodynamic drag coefficient	C_d	0.26
Vehicle frontal area	A_f	2.16 m^2
Rolling resistance coefficient	C_r	0.007
Wheel radius	R	0.3175 m
Density of air	ρ	1.2 kg/m^3
Acceleration due to gravity	g	9.81 m/s^2

The general structure of the model is shown in Fig. 9. The power demand from the wheels is split by a planetary gear set (PGS) to two motor-generators (MG) and an ICE. The ICE only outputs power to PGS but both MGs can work in either motor or generator mode. The MG1 works a generator to charge the battery when the state of charge (SOC) of the battery is low and outputs power as a motor to assist engine start process. The MG2 outputs power as a motor in normal driving while it retrieves power as a generator in regenerate braking process.

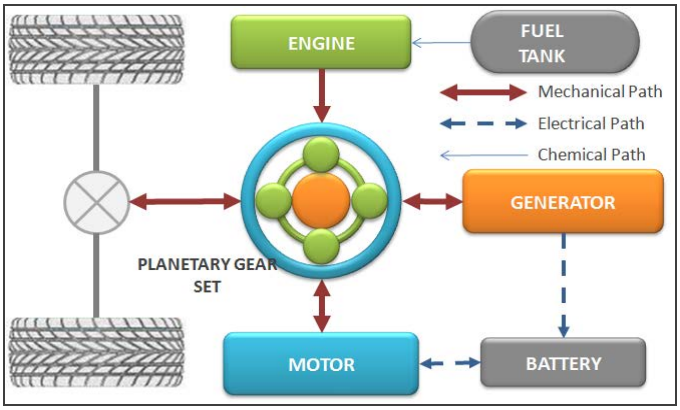

Fig. 9. Block diagram of a power-split HEV

Based on commands from the driving block, the power request is calculated and given as an input to a supervisory controller that contains a control strategy to minimize fuel consumption, as well as meet the power demand while maintaining the drivability [102]. Thus, the controller calculates the optimal power-split among the components with the power routed through the power-train to the wheels. The controller, under several criteria, determines the proportion of power on each component; (a) the power request from the wheel is met within the limit of the system, (b) the SOC of the battery is within preferred range, and (c) each component operates within desired efficiency zone. With these criteria, overall fuel efficiency of the PHEV is optimized based upon the equivalent fuel consumption minimization strategy (ECMS) [23]. A conventional vehicle model was also built for comparison with the PHEV. For comparability, the parameters of the conventional vehicle model were the same as the PHEV except the engine power was doubled to compensate for the fact that the conventional vehicle does not have an electric motor to provide additional power.

3.2.2 ECMS tuning

In (9) the equivalence factor *s* is an optimization parameter to be tuned and is related to the average powertrain efficiency in the future. The optimal value of *s* will be different for diverse driving profiles. That is, an *s* value that assures a close to optimal use of the battery energy for a particular driving cycle, can lead to poor use of the battery in others. This can be explained by the fact that the energy available for regeneration is a critical parameter that determines the amount of fuel required to recharge the battery and guarantee a sustaining operation. When addressing the issue of tuning the *s* coefficient, the energy control problem should be formulated as a global optimization problem and the cost function is defined as in (10).

$$\min_{s} \int_0^{t_f} \min_{P_{eng}, P_{em1}, P_{em2}} \dot{m}_{f,eq}(\tau) d\tau \tag{10}$$

According to this formulation, two approaches are proposed to adjust the equivalence factor in the ECMS. The first approach avoids the requirement of complete knowledge of the future conditions while the second approach allows adaptation to changes in the initially predicted velocity profile.

3.2.2.1 Approach 1

This approach is intended to get the maximum benefit by utilizing real-time roadway traffic data. The optimization is done for time horizons of equal lengths. Thus, the driving cycle is divided in sections according to the desired length. The optimization is done for each section to find the optimal control input *s(k)*, avoiding the requirement of

knowledge about the entire driving profile. The cost function for the optimal control problem at each time horizon becomes

$$\min_{s(k)} \int_{t_0+kT}^{t_0+T+kT} \min_{P_{eng},P_{em1},P_{em2}} \dot{m}_{f,eq}(\tau)d\tau \quad \forall \tau, k = 0,1,...,N-1 \tag{11}$$

Where t_0 is the time at the beginning of the current optimization horizon, T is the optimization horizon length, k is the optimization horizon number and N is the total number of optimization horizon windows.

3.2.2.2 Approach 2

In this approach the complete driving profile is used at first, but the optimal control input is recalculated and updated every T seconds for the remaining part of the predicted driving profile, i.e. from the current time to the estimated final trip time t_f. Thus, allowing adaptation to changes in the driving profile along the route. The optimization problem is stated as:

$$\min_{s(k)} \int_{t_0+kT}^{t_f} \min_{P_{eng},P_{em1},P_{em2}} \dot{m}_{f,eq}(\tau)d\tau \quad \forall \tau, k = 0,1,...,N-1 \tag{12}$$

3.2.3 Results

For comparison purposes, each approach was tested under the Urban Dynamometer Driving Schedule (UDDS) and the Federal Highway Driving Schedule (FHDS) each one repeated for 3600 s and assuming a 100% accurate speed profile prediction. Initially, a single optimal value for the *s* coefficient that minimizes the fuel consumption for each driving cycle was found. The results are summarized in Table 2.

Table 2. Fuel economy for single *s* value

Driving Cycle	S_opt	MPG
UDDS	4.4	55.45
FHDS	3.3	67.94

3.2.3.1 Approach 1

According to the results in Table 3, initially the fuel economy improves for bigger time windows. This suggests that bigger time windows would yield better results. However, for time horizons 600 s, 900 s and 1200 s the MPG value was smaller than the value obtained for 300 s. For time windows less than 300 s, there is not enough opportunity to take full advantage of the battery energy. While for time windows greater than 300 s, there is a large variation in the driving profile, thus, a constant value of S is not enough to optimize the fuel economy. Consequently, 300 s corresponds to the optimal value for the time horizon length. That means that it is required to have a prediction of the speed profile for the upcoming 300 s at each instant of time.

Table 3. Fuel economy usign approach 1 to tune the *s* coefficient

Driving Cycle	Time horizon [s]	MPG	Improvement %
UDDS	60	53.52	-4.89
	120	56.34	0.11
	300	58.68	4.28
	600	56.67	0.70
	900	56.76	0.86
	1200	56.37	0.17
FHDS	60	66.78	-1.69
	120	67.99	0.076
	300	68.71	1.13
	600	68.43	0.72
	900	68.04	0.14
	1200	67.86	-0.11

It is also important to highlight that the improvement percentage is bigger for the UDDS cycle, which is consistent with the fact that there is more variation in the driving conditions for this driving cycle than for the FHDS cycle.

3.2.3.2 Approach 2

According to the results summarized in Table 4, this approach yields better fuel economy than approach 1, due to the use of the remaining part of the driving cycle and the continuous updating of the coefficient *s*. It is also important to point out the lower MPG values obtained for bigger updating time for the *s* coefficient which suggest in this approach a small window size is better to get maximum benefits.

Table 4. Fuel economy using approach 2 to tune the *s* coefficient

Driving Cycle	Updating time window[s]	MPG	Improvement %
UDDS	60	60.41	6.85
	120	60.35	6.76
	300	59.20	4.95
FHDS	60	69.58	2.35
	120	69.32	1.98
	300	69.05	1.60

The results demonstrates that model predictive control techniques are useful to reduce energy consumption in HEV's using the ECMS algorithm as the base of its energy control strategy, while keeping its potential for real time implementation. In the first approach, roadway traffic prediction data is sent to the supervisory controller to tune the ECMS algorithm for a particular horizon time length. The results showed that 300 s is the optimal time horizon size, resulting in fuel economy improvements of 1.13 to 4.28%

when compared to the case of a constant *s* value for the complete predicted driving cycle. In the second approach, the control input is periodically recalculated, allowing adaptation to changes in the predicted driving profile along the entire trip. The simulations revealed that 60 seconds becomes an optimal updating time for this case, with fuel economy improvements of 2.35 to 6.85%.

3.3 ECMS tuning through statistical analysis of engine operating points

This approach starts with the use of the Willans-line model to parameterize the internal combustion engine (eng) which allows the use of the intrinsic engine efficiency to find a suitable range for the equivalent factor s optimal value. Once the proper range is defined, it is possible to find the optimal value through analysis of the operating points' distribution. The powertrain model used for this work is discussed next.

3.3.1 Parallel through the road hybrid electric vehicle model

In a parallel HEV the engine and the electric motor are habilitated to provide power independently or simultaneously. This combination adds a degree of freedom to the system which allows finding an optimal distribution of the power. In the conventional parallel configuration, the electric motor and the engine are mechanically coupled in order to allow its simultaneous operation. However, as it is illustrated in Fig. 10, for the parallel through the road configuration the coupling is achieved through the road.

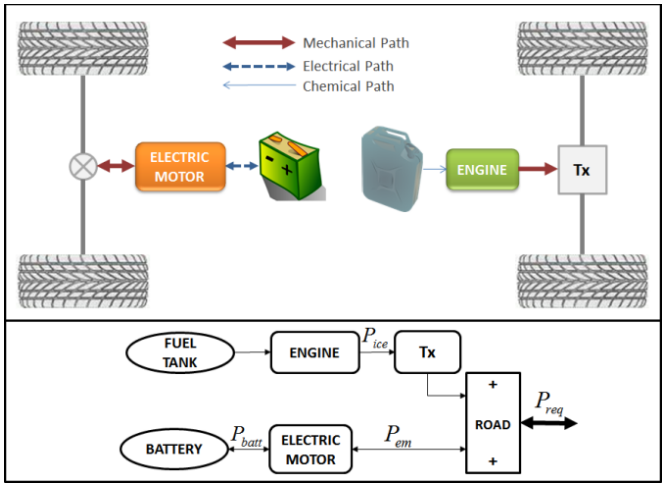

Fig. 10. Schematic representation of a parallel through the road HEV

Therefore, the requested power P_{req} is a function of the engine power P_{eng} and the electric machine power P_{em} :

$$P_{req}(t) = \eta_t P_{eng}(t) + \beta P_{batt}(t) \tag{13}$$

Where η_t is the transmission efficiency and β is the efficiency of the electro-mechanical path which depends on the direction of the electrical energy flow. The model was implemented using a forward-looking approach and utilizing the engine and the electric motor efficiency maps. The vehicle dynamics is defined by eq. (14).

$$\dot{v} = \frac{1}{m_v}(f_t - f_a - f_g - f_r) \tag{14}$$

Where $f_a = \rho_{air} C_d A_f v^2$, $f_g = m_v g \sin(\alpha)$, $f_r = C_r m_v g \cos(\alpha)$, v is the longitudinal speed, m_v is the mass of the vehicle, f_t is the traction force of the vehicle [N], ρ_{air} is the density of air [kg/m3], C_d is the drag coefficient, A_f is the vehicle

frontal area, g is the acceleration due to gravity [m/s2], α is the road grade and C_r is the rolling resistance coefficient.

The battery was modeled by using a first order approximation in which the state-of-charge (SOC) dynamics is described by eq. (15).

$$\dot{SOC} = -\frac{V_{oc} - \sqrt{V_{oc}^{\ 2} - 4P_{batt}R_{\text{int}}}}{2R_{\text{int}}Q_{batt}} \tag{15}$$

Where V_{oc} is the battery open-circuit voltage, P_{batt} is the battery power, R_{int} is the battery internal resistance and Q_{batt} the battery capacity. The main parameters of the vehicle are presented in Table 5.

Table 5. Main parameters of the vehicle

Parameter	Value
Vehicle mass [Kg]	2000
Aerodynamic drag coefficient	0.4160
Vehicle frontal area [m^2]	2.82
Rolling resistance Coefficient	0.012
Tire radius [m]	0.3305
Engine max Power [kW]	110
Motor max Power [kW]	25
Battery capacity [Ah]	6.5

3.3.2 Willans-line model

The Willans-line model provides a simplified representation of the engine torque and efficiency. It has been shown it can approximate the real engine behavior with significant precision [103]. Defining P_{chem} as the chemical power available in the fuel, the engine power can be defined as in Eq. (16).

$$P_{eng} = \omega_{eng}T_{\ eng} = \eta(\cdot)P_{chem} = \eta(\cdot)\dot{m}_f Q_{lhv} \tag{16}$$

Where ω_{eng} is the engine angular speed, T_{eng} is the engine effective torque, $\dot{m}_f$ is the fuel mass flow rate, Q_{lhv} is the fuel low heating value and $\eta(\cdot)$ is the engine efficiency that depend on different parameters.

According to the Willans-line approximation, illustrated in, the engine's efficiency can be assumed as an affine representation, relating the power and the fuel mass flow rate. Such relation is defined by Eq. (17).

$$P_{eng} = e(\omega)P_{chem} + P_{loss}(\omega) = e(\omega)\cdot\dot{m}_f Q_{lhv} + P_{loss}(\omega) \tag{17}$$

Where $e(\omega)$ is the intrinsic fuel conversion efficiency and $P_{loss}(\omega)$ are the power losses due to air pumping, mechanical friction and magnetic phenomena. From Eq. (17), the engine fuel flow rate is defined as:

$$\dot{m}_{f,eng} = \frac{P_{eng} - P_{loss}}{e\cdot Q_{lhv}} \tag{18}$$

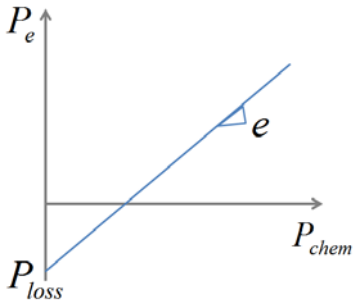

Fig. 11. Willans line model affine representation

The intrinsic fuel conversion efficiency is a parameter to be determined and it depends on engine parameters like the air to fuel ratio, the exhaust gas recirculation,

spark timing, etc. Moreover, this parameter, as well as P_{loss}, are nonlinear and can be represented as a function of the engine speed and torque. However, the dependence on the torque can be neglected [103]. In particular, if full-load conditions are avoided equations (19) and (20) hold.

$$e(\omega) \approx (a_{00} + a_{01}\omega + a_{02}\omega^2) \tag{19}$$

$$P_{loss}(\omega) \approx (P_{loss0} + P_{loss2}\omega^2) \tag{20}$$

Fig. 12 illustrates the Willans lines for the 110 kW, 1.9-L Diesel engine used in this work. The corresponding intrinsic efficiency is presented in Fig. 13.

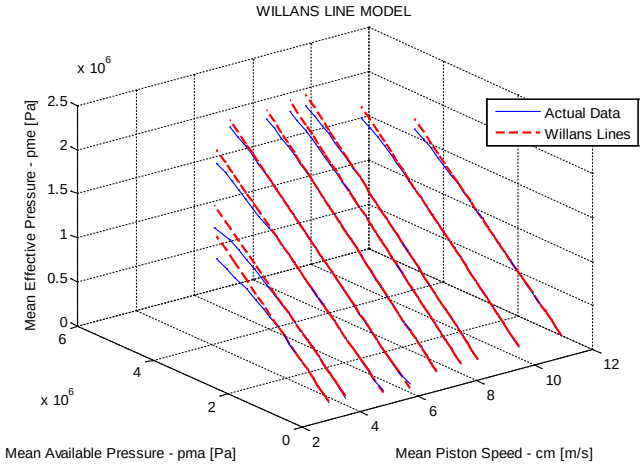

Fig. 12. Willans lines for a 110 Kw, 1.9L Engine

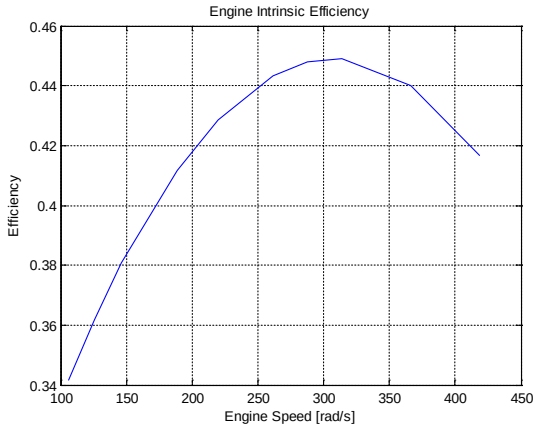

Fig. 13. Intrinsic fuel conversion efficiency for a 110 Kw, 1.9L Engine

3.3.3 Equivalent consumption minimization strategy – ECMS

Recall the optimization problem stated in section 3.1:

$$\min_{\{P_{eng}(t),P_{em_i}(t)\}} \dot{m}_{f,eq}(t) \tag{21}$$

Subject to:

$$P_{req}(t) = P_{eng}(t) + P_{em1}(t) - P_{em2}(t)$$
$$0 < SOC_{\min} \le SOC \le SOC_{\max} < 1$$
$$0 \le P_{eng}(t) \le P_{eng,\max}(t)$$
$$0 \le \omega_{eng}(t) \le \omega_{eng,\max}(t)$$
$$0 \le T_{eng}(t) \le T_{eng,\max}(t)$$
$$P_{em,\min}(t) \le P_{em}(t) \le P_{em,\max}(t)$$
$$\omega_{em,\min}(t) \le \omega_{em}(t) \le \omega_{em,\max}(t)$$
$$T_{em,\min}(t) \le T_{em}(t) \le T_{em,\max}(t)$$

Where $\dot{m}_{f,eq}(t) = \dot{m}_{f,\text{eng}}(t) + \dot{m}_{f,eq,batt}(t)$ is the equivalent fuel flow rate, $\dot{m}_{f,eng}$ is the engine's fuel flow rate and $\dot{m}_{f,eq,batt}$ represents an equivalent fuel flow rate related to the use of the battery power. For the general case, and assuming the equivalence factor s

remains constant for the charging and discharging case, the equivalent battery fuel flow rate is a function of the equivalence factor s, the battery power P_{batt} and the Q_{lhv} as in (22).

$$\dot{m}_{f,eq,batt} = s \cdot \frac{\beta \cdot P_{batt}}{\eta_t \cdot Q_{lhv}} \tag{22}$$

This local optimization is known as the equivalent consumption minimization strategy (ECMS) and constitutes the base of the energy management strategy used here.

3.3.4 Alternative ECMS Implementation

The Willans-line model is utilized to calculate the engine fuel consumption. Thus, assuming that the power request P_{req} is a function of the engine power P_{eng} and the battery power P_{batt}, as defined in Eq.(13), and utilizing Eq. (18), an alternative equation for the engine fuel flow rate is found (Eq.(23)). To simplify the analysis, all the efficiencies are assumed equal to 1.

$$\dot{m}_{f,eng} = \frac{P_{req} - \beta P_{batt} + \eta_t P_{loss}}{e \eta_t Q_{lhv}} \tag{23}$$

Then, the equivalent fuel consumption is defined by Eq. (24). Note that, for a particular speed and power request, the first two terms in (24) are constant. Hence, the variables in the last term will define the conditions to have minimum equivalent fuel consumption.

$$\dot{m}_{f,eq} = \frac{P_{req}}{e(\omega)\eta_t Q_{lhv}} + \frac{P_{loss}}{e(\omega) Q_{lhv}} + \frac{\beta P_{batt}}{\eta_t Q_{lhv}} \left(s - \frac{1}{e(\omega)} \right) \tag{24}$$

Thus, assuming $P_{req} > 0$ and for given s, ω and $e(\omega)$, the trend of $\dot{m}_{f,eq}$ depends on the relation between s and $e(\omega)$ as follows:

- ✓ If $S > \frac{1}{e(\omega)} \rightarrow \begin{cases} P_{bat} > 0 \rightarrow m_{f,eq} \uparrow \\ P_{bat} < 0 \rightarrow m_{f,eq} \downarrow \\ P_{bat} = 0 \rightarrow m_{f,eq} = const. \end{cases}$
- ✓ If $S < \frac{1}{e(\omega)} \rightarrow \begin{cases} P_{bat} > 0 \rightarrow m_{f,eq} \downarrow \\ P_{bat} < 0 \rightarrow m_{f,eq} \uparrow \\ P_{bat} = 0 \rightarrow m_{f,eq} = const. \end{cases}$

For example, for $P_{bat} > 0$, this dependency is illustrated in Fig. 14.

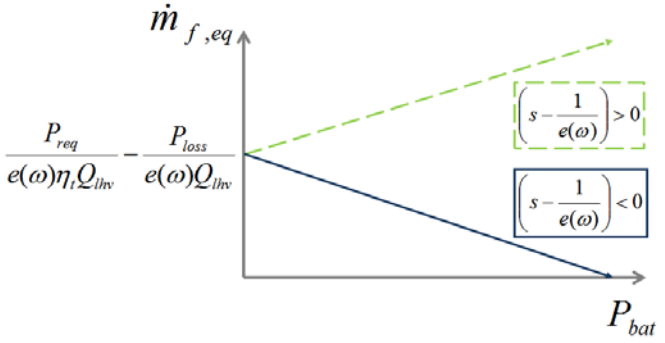

Fig. 14. Fuel flow rate $\dot{m}_{f,eq}$ trends

Consequently, to minimize the equivalent fuel consumption, if $s > 1/e(\omega)$, P_{bat} has to be negative, i.e. engine is used to recharge the battery (recharging mode). In the contrary case, if $s < 1/e(\omega)$, P_{bat} has to be positive, i.e. the battery is providing power. This implies the speed value(s) for which $s = 1/e(\omega)$, will divide the engine efficiency map in different regions. For each region the operating points will correspond to a particular mode of operation, i.e. recharging or discharging.

Accordingly, different values of s will produce a different distribution of the recharging and discharging regions on the efficiency map. This behavior is illustrated in Fig. 15.

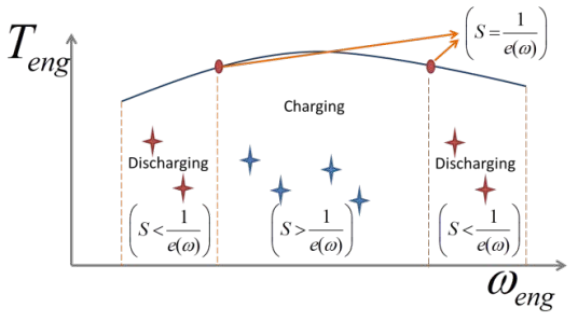

Fig. 15. Relationship between the equivalence factor and the fuel intrinsic efficiency

3.3.5 Operating points distribution graphic analysis

It is important to note that the stated relationship between the equivalence factor s and the fuel conversion intrinsic efficiency $e(\omega)$, allows defining a feasible range for the optimal value of s, reducing the search range and therefore the optimization time.

For the case of the intrinsic efficiency plot in Fig. 13, the feasible range for the optimum value of *s* is [2.2161, 2.8652].

Moreover, it is possible to take advantage of the particular distribution of the points to find a sustaining optimal value for *s* which produces a sustained used of the battery. This means to satisfy the condition SOEstart ≈ SOEend. Note that, to meet this condition, the net energy content of the electric machine operating points must be zero or, very close to zero.

To have a better understanding of the operating points distribution, the simulator was initially tuned for the FUDS driving cycle and by using a basic iterative tuning

approach it was found that the sustaining-optimal *s* value for the FUDS is 2.23233. Then, six different *s* values, contained in the previously defined feasible range, were chosen and the operating points for each one were analyzed.

The previously stated division of the operating points in the engine efficiency map, for the optimal *s* value, is shown in Fig. 16. The operating points on the engine map are divided into two regions which are separated at the speed value correlated to the point $S = 2.23233 = 1/e(\omega)$, thus, $\omega = 282$. The operating points located to the left belong to discharging points while the points located to the right are recharging points and are placed at higher efficiency values.

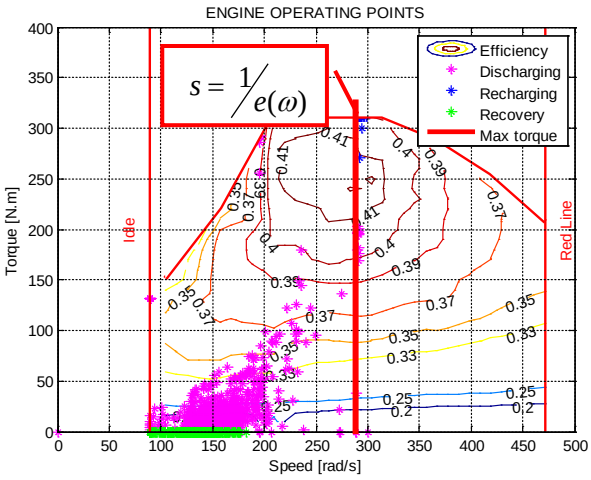

Fig. 16. Engine Operating points for FUDS, S=2.23233

Fig. 17 shows that the electric machine operating points are mainly concentrated in the areas of higher efficiency. The SOE pattern in Fig. 18 confirms that sustainability is achieved with the tuned *s* value.

The additional six values of *s* used for analysis are 2.22, 2.228, 2.236, 2.244, 2.252, 2.26, and the respective engine operating points are shown in Fig. 19.

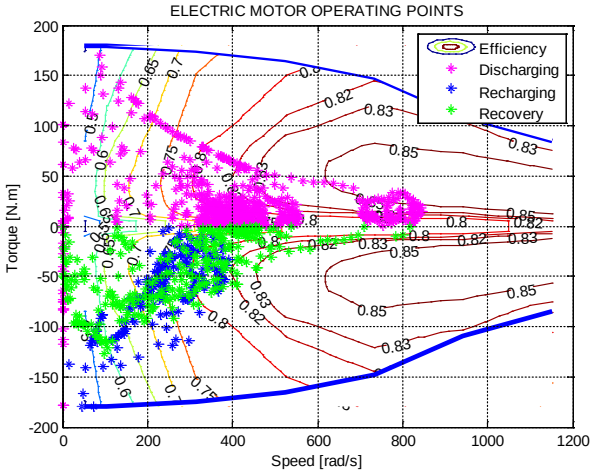

Fig. 17. Electric Motor Operating points for FUDS, S=2.23233

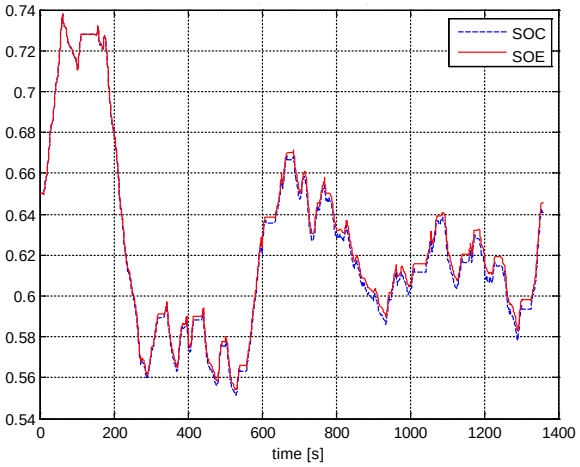

Fig. 18. SOE and SOC patterns for FUDS, S=2.23233

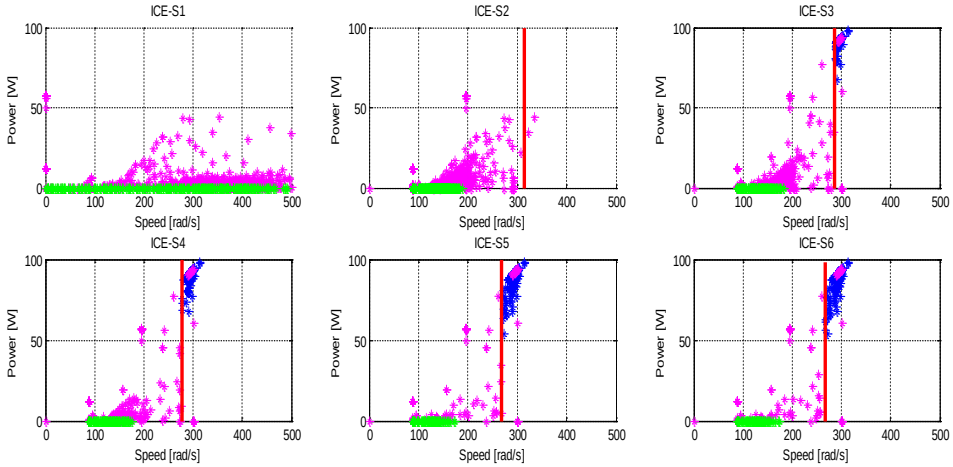

Fig. 19. Engine Operating Points for different values of S (pink: discharging, blue: recharging, Green: recovery)

Between S1 and S2 (Fig. 19), the operating points are only for discharging condition. From S2 to S3, there is a significant difference since the recharging points appear on the map. This implies that the sustaining s value must be contained inside this range, which can be confirmed with the tuned value previously found. From S3 to S6, the distribution moves to the right showing an increment of the recharging points. Note that from S3 to S6 some outliers are present which are due to limitations in the machines. Such outliers are not present for the case of the sustaining s value (refer to Fig. 16). According to the histograms in Fig. 20, the operating points corresponding to the values of s which allow recharging of the battery, follow a bimodal distribution

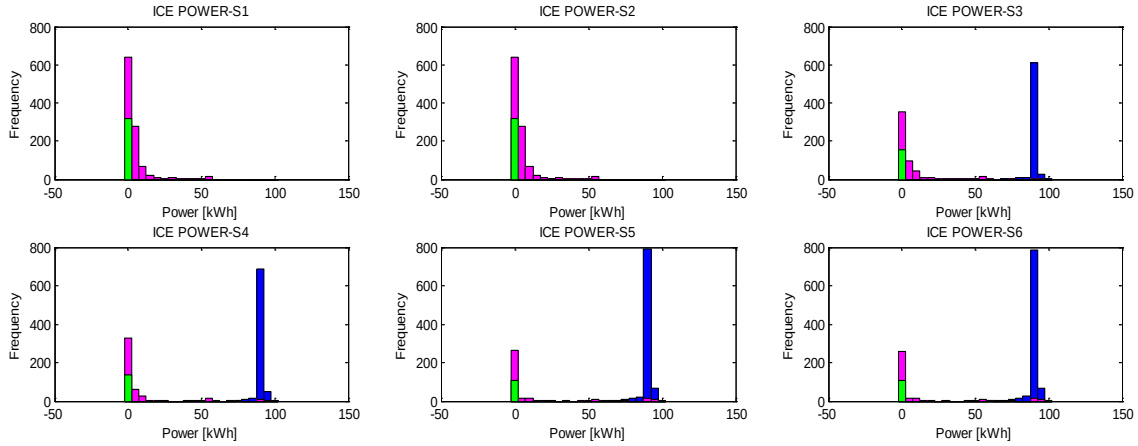

Fig. 20. Histograms for Engine Operating points (pink: discharging, blue: recharging, Green: recovery)

The operating points for the case of the electric motor are shown in Fig. 21. To have a sustaining battery use, the electric motor operating points need to have a net energy balance, i.e., the net summation of the points must be zero or very close to zero.

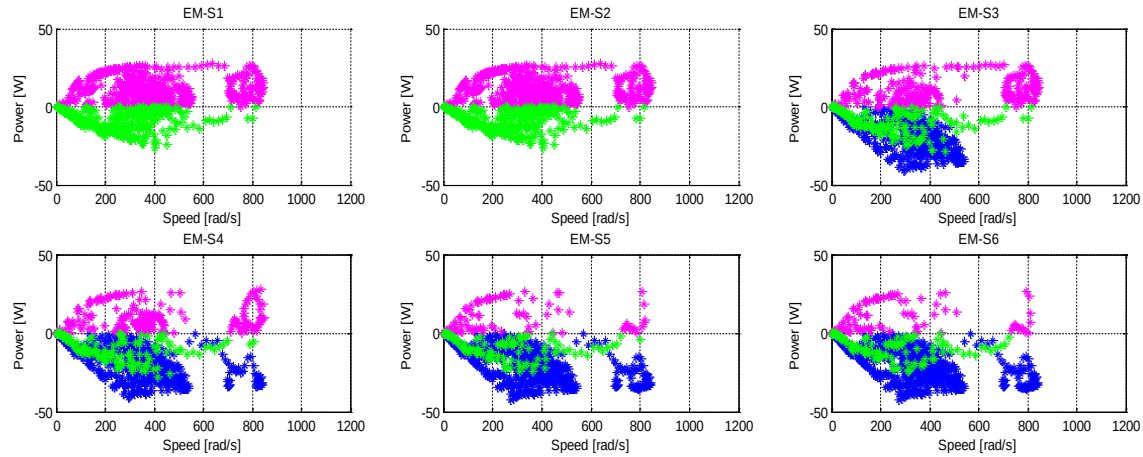

Fig. 21. Electric motor operating points for different values of s (pink: discharging, blue: recharging, green: recovery)

For S1 and S2, there is over-discharging which means, the final SOE is lower than the initial SOE. In contrast, for S3 to S6, there is over-charging of the battery. Hence, the final SOE is bigger than the initial SOE. Note that the distribution of the operating points remains relatively constant for S1 and S2 and for S4 to S6.

The histograms in Fig. 22 show the trend of the electric motor power. Note that as the value of *s* increases the distribution is skewed to the left due to the increment of the recharging power. For a sustaining operation, it is required to have a mean power equal to zero.

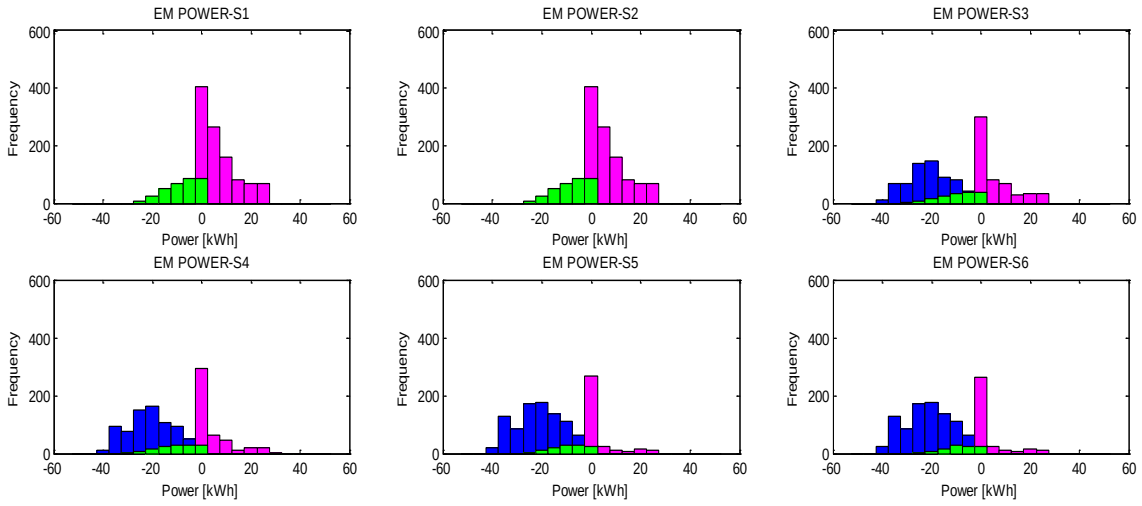

Fig. 22. Histograms for electric motor operating points

3.3.6 Operating points distribution net energy analysis

To complement the graphic analysis and have a better understanding of the operating points trends due to changes on the *s* value, the net engine and electric motor energy consumed was calculated for each *s* value according to equations (25) and (26).

$$E_{ICE,S_i,net} = E_{ICE,S_i,dis} + E_{ICE,S_i,chg} \quad (25)$$

$$E_{EM,S_i,net} = E_{EM,S_i,dis} + E_{EM,S_i,chg} + E_{EM,S_i,rec} \quad (26)$$

Then, the net delta energy (ΔE) and the net delta energy total (ΔE_{total}) was determined for each consecutive pair of *s* values using equations (27), (28) and (29).

$$\Delta E_{ICE,S_i,S_{i+1}} = E_{ICE,S_{i+1},net} - E_{ICE,S_i,net} \quad (27)$$

$$\Delta E_{EM,S_i,S_{i+1}} = E_{EM,S_{i+1},net} - E_{EM,S_i,net} \quad (28)$$

$$\Delta E_{total,S_i,S_{i+1}} = \Delta E_{ICE,S_i,S_{i+1}} - \Delta E_{EM,S_i,S_{i+1}} \quad (29)$$

From the results reported in Table 6, it is observed that for the range of *s* containing the optimal sustaining value, there is a change of sign in the final delta SOE value.

Table 6. Operating points Net energy analysis

S Values	S1-S2	S2-S3	S3-S4	S4-S5	S5-S6
	2.2200,2.2280	2.2280,2.2360	2.2360,2.2440	2.2440,2.2520	2.2520,2.2600
ICE Net SX Energy [kJ]	*1877.80*	*1878.10*	*62866.10*	*74351.00*	*88822.90*
ICE Net SX+1 Energy [kJ]	*1878.10*	*62866.10*	*74351.00*	*88822.90*	*89043.50*
ICE ΔE [kJ]	***0.30***	***60988.00***	***11484.90***	***14471.90***	***220.60***
EM Net SX Energy	*4758.90*	*4758.80*	*-11704.20*	*-15076.30*	*-19037.28*
EM Net SX+1 Energy	*4758.80*	*-11704.20*	*-15076.30*	*-19037.28*	*-19114.51*
EM ΔE [kJ]	***-0.10***	***-16463.00***	***-3372.10***	***-3960.98***	***-77.23***
Final Delta SOE SX	*0.51*	*0.51*	*-1.14*	*-1.47*	*-1.84*
Final Delta SOE SX+1	*0.51*	*-1.14*	*-1.47*	*-1.84*	*-1.84*
ΔE_{total} [kJ]	**0.20**	**44525.00**	**8112.80**	**10510.92**	**143.37**

Thus, for lower values of *s* the difference between the final and initial delta SOE is positive. As *s* increases and the optimal sustaining value is reached, the difference will tend to zero. Finally, for further increments in *s* the difference becomes negative,

resulting in over-charging of the battery. Accordingly, the optimal sustaining s value should be between the two for which a change of sign is given, i.e $s2$ and $s3$ in Table 6.

Furthermore, as seen in Fig. 23, it was found that the net delta energy total has a maximum for the s pair which contains the Optimal Sustaining s_{opt} value. The following observations are valid for each region:

- ✓ *Over-discharging region*: the net delta energy is very close to cero.
  - The energy values for two different s are very close to each other. This is valid for both, the engine and the electric motor, so they cancel each other.
  - The engine is hardly used. Thus its energy use is very low.
- ✓ *Over-charging region:* the net delta energy is a little higher than the over-discharging, but still lower.
  - In this case the values continue being very close to each other, although the engine is being used to recharge the electric machine, its net energy is still small. The total energy is even lower since the savings from recharging the electric machine are subtracted.
- ✓ *Sustaining region:* The region containing the optimum will have a change of sign in the electric motor net energy, and a significant jump in the engine net energy due to its additional use to recharge the battery. Thus it will contain maximum net delta energy total (Fig. 23).

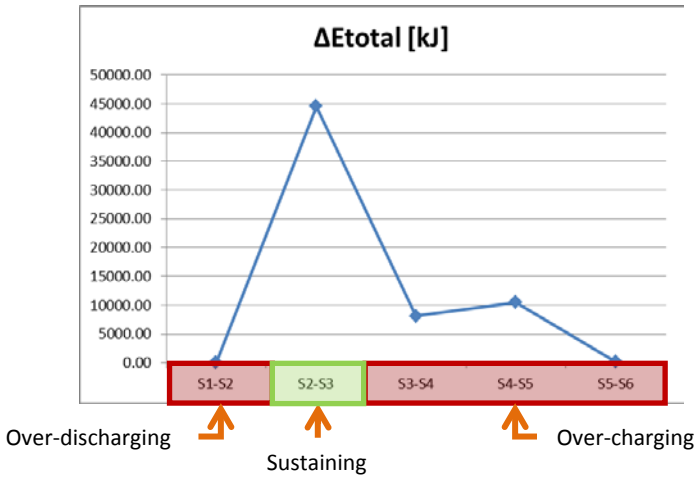

Fig. 23. Delta energy total – FUDS

The analysis was repeated for FHDS and US06 using different values of *s*. For all the evaluated cases the results were consistent with the mentioned observations.

3.3.7 Proposed Tuning approaches

Two approaches are proposed to solve numerically the problem. The first approach is based in the operating points comparison and net delta energy total. The second approach is based in the final delta SOC and energy required to achieve charge sustainability.

3.3.7.1 Approach 1

The goal on this approach is to find a pair of S values which produces the maximum net delta energy total, while the difference between the two is less than a previously defined threshold.

The optimization problem can be stated as in (30).

$$J = \max_{S_i, S_{i+1}} \Delta E_{total, S_i, S_{i+1}} \tag{30}$$

The algorithm is summarized in Table 7.

Table 7. Algorithm for approach 1

Inputs	Outputs
S1, S2, S3	ΔE_{total}, Sopt1, Sopt2
1. Define the desired threshold (δ) or minimum desired resolution for *s* 2. Choose 3 values for *s* in the probable region (Smin, Smin+(Smax-Smin)/2, Smax) 3. Calculate intrinsic efficiency and use interpolation to find ω 4. Run simulator for each *s* value and save relevant data 5. Calculate ΔE_{total} for consecutive pairs of *s* 6. Choose the *s* pair producing the maximum ΔE_{total} and save the new Smin and Smax values 7. Repeat steps 2 to 6 until the threshold defined in step 1 is reached	

To achieve a final SOE value very close to zero for the FUDS driving cycle, a resolution of at least 0.00001 is required. If the entire "feasible" *s* range is gridded, 700004 iterations are required to achieve such resolution. However, if the algorithm described in Table 7 is used, only 0.059% of those iterations are needed.

The plot in Fig. 24 illustrates the convergence rate of the approach 1.

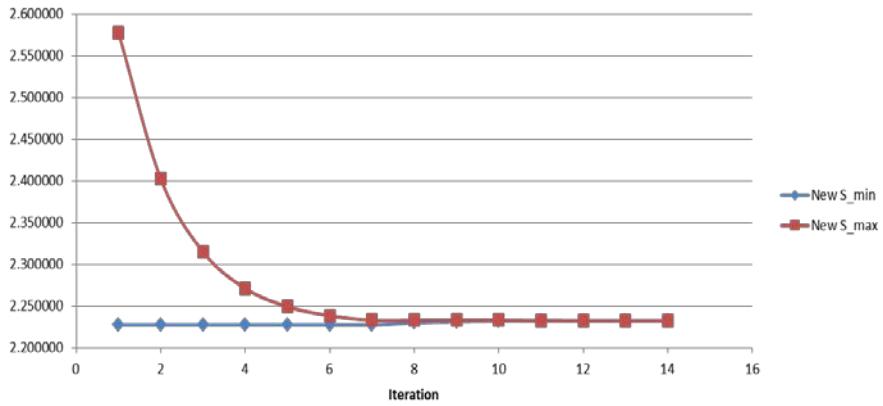

Fig. 24. Convergence rate for Approach 1

3.3.7.2 Approach 2

This approach attempts to use the histograms information along with the final SOE to find the value of *s* which will produce a battery charge sustaining operation. The algorithm is summarized in Table 8.

Table 8. Algorithm for approach 2

Inputs	Outputs
S1, S2, S3	ΔE_{total}, Sopt1, Sopt2
1. Define the desired threshold (δ) $\boldsymbol{\delta}$) or minimum desired resolution for ΔSOE 2. Select S=Smin+(Smax-Smin)/2 3. Run simulator 4. Find final ΔSOE and calculate the corresponding energy value 5. Add or subtract bins (counts*width of bins) to achieve final ΔSOE=0 and determine the new ω 6. Use interpolation to find the intrinsic efficiency which corresponds to the ω found in step 4. 7. Calculate the S value corresponding to the intrinsic efficiency found in step 5. 8. Repeat steps 3 to 7 until $\Delta SOE \leq \delta$	

In this case, to achieve a resolution of 0.001 by gridding the entire "feasible" *s* range, around 700 iterations are needed. However, only 0.57% of such iterations are required for approach 2, which corresponds to 16% of the iterations required for approach 1. The plot in Fig. 25 illustrates the convergence rate of the approach 2.

The results presented in this section, have been consistent with the results obtained for the FHDS and US06 cycles.

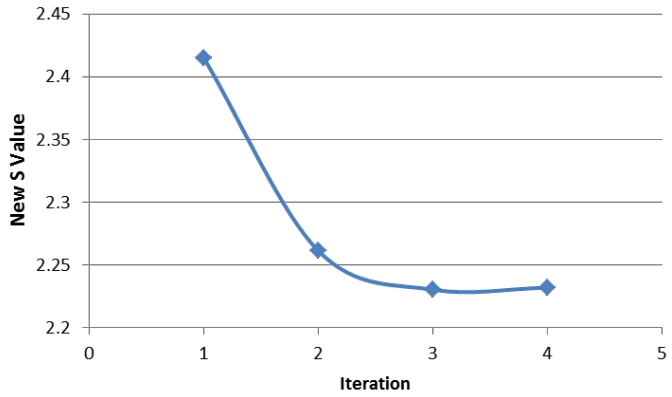

Fig. 25. Convergence rate for approach 2

3.3.8 Concluding Remarks

An alternative approach for the ECMS strategy implementation has been proposed. The strategy involves the use of the Willans-line approximation to estimate the engine fuel consumption. Although the strategy still requires the tuning of the equivalent factor, the use of the intrinsic efficiency and its stated relation to the equivalence factor, allows finding a feasible region for the optimal value of s. Thus, it speeds up the tuning process. Furthermore, the new operating points distribution is useful to facilitate the real-time tuning of the strategy.

For the proposed numerical solutions, it was found that the number of iterations required to find an optimal sustaining value for *s*, can be reduced by up to 0.057% the total number of iterations required with a standard iterative approach.

CHAPTER FOUR

4 DRIVING PROFILE OPTIMIZATION AND ECO-DRIVING

4.1 Effects of smoother driving profile for conventional and PHEV powertrains[2]

With the goal of assess the benefits of having smoother speed profiles, the models of a conventional vehicle and a PHEV were implemented in Matlab/Simulink. Then, for the PHEV an energy management strategy was implemented and finally, a driving cycle optimization routine was developed. By combining those elements we obtained a two level optimization system. In a low level, the PHEV energy consumption is optimized by using the ECMS. And, in a high level, the driving profile predicted from information obtained through intelligent transportation systems is optimized to avoid frequent acceleration/deceleration paths. For details regarding the in-vehicle optimization for the plug-in hybrid electric vehicle, refer to the content in section 3.1

4.1.1 Driving profile optimization

The driving profile optimization was implemented following a basic approach in which the vehicle speed v within an optimization horizon T is defined as:

$$v = f(t) = \int a(t)dt \tag{31}$$

For each optimization horizon, the initial speed is fixed to the speed at the end of the previous optimization horizon and the distances are the same before and after the optimization:

[2] Based upon work supported by the National Science Foundation (NSF) and under Grant No. 0928744. Any opinions, findings, and conclusions or recommendations expressed in this material are those of the author(s) and do not necessarily reflect the views of the National Science Foundation.

$$f(t_0) = v_0 \tag{32}$$

$$f(t_0 + T) = v_p \tag{33}$$

$$\int_{t_0}^{t_0+T} f(t)dt = s \tag{34}$$

Where t_0 is the time at the beginning of the current optimization horizon, T is the length of the optimization horizon, v_0 is the vehicle speed at the beginning of the current optimization horizon, v_p is the predicted speed at time $t_0 + T$, and s is the distance between the current position and the predicted position at $t_0 + T$. The acceleration is assumed constant when the driver is following the driving cycle:

$$a = \frac{v_p^2 - v_0^2}{2s} \tag{35}$$

And the vehicle speed becomes:

$$v = f(t) = v_0 + at \tag{36}$$

To meet the constraints (33) and (34), the actual time for the vehicle to travel the distance s may be different from the optimization horizon. However, the travel time is not the primary consideration and the differences in travel time obtained with the testing results are within an acceptable range.

4.1.2 Results

Two tests were conducted to analyze the effects of smoother driving patterns.

4.1.2.1 Test 1: model validation

The fuel economy of the PHEV was estimated for standard driving cycles and the results were compared to results obtained with Dynamic programming published by Liu and Peng [104]. Errors of less than 6% confirmed the validity of the results (Table 9).

Table 9. Fuel consumption for standard driving cycles

Standard Driving cycle	MPG (Dynamic Programing)	MPG (PHEV Simulator)	Error
UDDS	57	56.87	0.23%
FHDS	67	63.02	5.94%

4.1.2.2 Test 2: driving profile optimization performance

The velocity profiles were optimized and the fuel economy was estimated for each vehicle. Three different optimization horizon sizes were evaluated for the conventional and the PHEV: 30 s, 60 s and 120 s. The performance in terms of mpg and the corresponding improvement percentage is shown for optimization horizons in Table 10. Improvements are seen with respect to the fuel efficiency of conventional vehicles on the original simulation cycles. Although the performance varies among driving cycles with a few of them exhibiting a slight decrease in efficiency, the average improvement in fuel efficiency is significant: 54% for the 30 s horizon, 78% for the 60 s horizon and 86% for the 120 s horizon. A better performance was achieved for the PHEV by integrating the cycle optimization algorithm in the PHEV power management system (Table 11). Over a 100% average improvement was obtained for all optimization horizons compared to the PHEV without cycle optimization. Like conventional vehicles, the 120 s horizon has the highest average fuel efficiency of 63.37 mpg, compared to 62.94 mpg for 60 s and 62.93 mpg for 30 s.

Table 10. Driving cycle optimization performance for conventional vehicle

	Original (mpg)	OP30 (mpg)	Improvement (%)	OP60 (mpg)	Improvement (%)	OP120 (mpg)	Improvement (%)
1	18.82	33.36	77.2	43.44	130.8	44.45	136.1
2	17.80	14.91	−16.2	15.56	−12.6	12.15	−31.7
3	12.64	22.62	79.0	23.12	82.9	27.89	120.6
4	12.75	19.20	50.5	23.28	82.5	24.49	92.0
5	15.14	29.55	95.1	40.12	165.0	48.23	218.5
6	10.33	11.58	12.1	13.97	35.2	14.38	39.2
7	13.22	14.82	12.1	14.13	6.9	11.40	−13.8
8	12.45	21.19	70.2	22.74	82.6	25.12	101.8
9	11.46	7.60	−33.7	7.13	−37.8	9.61	−16.2
10	8.09	10.24	26.6	10.51	29.8	9.05	11.8
Average	13.64	20.99	53.9	24.24	77.7	25.36	85.9

Table 11. Driving cycle optimization performance for PHEV

	Original (mpg)	OP30 (mpg)	Improvement (%)	OP60 (mpg)	Improvement (%)	OP120 (mpg)	Improvement (%)
1	31.81	64.15	101.6	72.55	128.0	67.02	110.6
2	59.36	65.10	9.7	71.31	20.1	66.53	12.1
3	38.06	64.99	70.8	67.99	78.6	59.37	56.0
4	34.20	60.08	75.7	55.44	62.1	57.18	67.2
5	23.26	61.00	162.2	54.23	133.1	74.69	221.1
6	24.04	56.12	133.4	57.33	138.4	64.37	167.7
7	33.47	43.43	29.7	68.66	105.2	35.74	6.8
8	25.99	80.83	211.0	70.28	170.4	65.27	151.1
9	28.72	49.80	73.4	40.09	39.6	43.12	50.1
10	21.62	65.28	201.9	68.05	214.7	64.45	198.1
Average	29.27	62.93	114.9	62.94	115.0	63.37	116.5

4.2 Eco-driving for electric vehicles

To analyze the effects of less aggressive driving in electric vehicles, the driving profile optimization framework proposed by Malikopoulos and Aguilar [40] for conventional gasoline-powered vehicles was adapted to the case of an electric bus. It uses a base driving profile for a particular schedule and finds the energy-optimal driving profile which will yield lower energy consumption for that route. The Optimization routine is composed by three main processes: (1) Energy consumption estimation, (2) Optimization problem solution and, (3) Finding the optimal driving profile.

4.2.1 Energy consumption estimation

To estimate the energy consumption of the electric bus over a defined driving route, the base normal driving profile illustrated in Fig. 26 was used. It was obtained experimentally from an actual electric bus through the can data. Additional relevant data related to the electric bus performance was also recorded to obtain a meta-model for the fuel consumption.

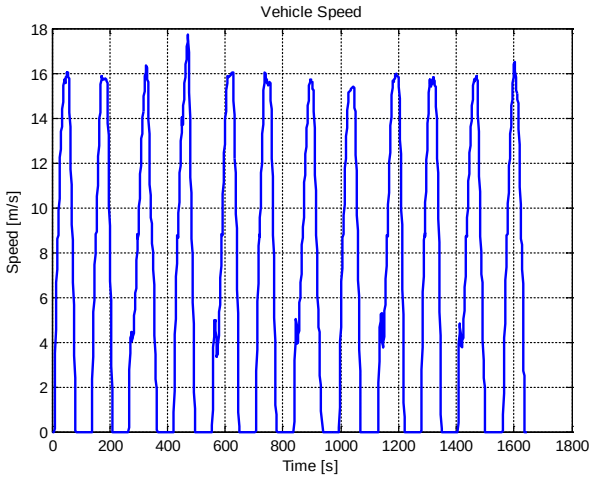

Fig. 26. Base normal driving profile

The meta-model allows estimating the instantaneous electrical power P as a function of the speed v, acceleration a a nd grade θ. Using a meta-model avoids the requirement of more complex models or simulations, speeding up the solution of the optimization problem. Since it is wanted to estimate the instantaneous power consumption, the equation for the meta-model (Equation (37)) is chosen to be similar in structure to the vehicle dynamics equation.

$$P = f(v,a) = \alpha_1 \cos(\theta)v + \alpha_2 \sin(\theta) + \alpha_3 va + \alpha_4 v^3 \tag{37}$$

Where α_i are the linear coefficients correlating the power with the speed and acceleration. In order to find these coefficients, the system of Equation (38) is used and solved for $\overline{X}$. To find the solution, the experimental data for the base normal driving profile is used.

$$\overline{Y} = \overline{A}\overline{X} \tag{38}$$

Fig. 27 illustrates the meta-model for the base normal driving profile.

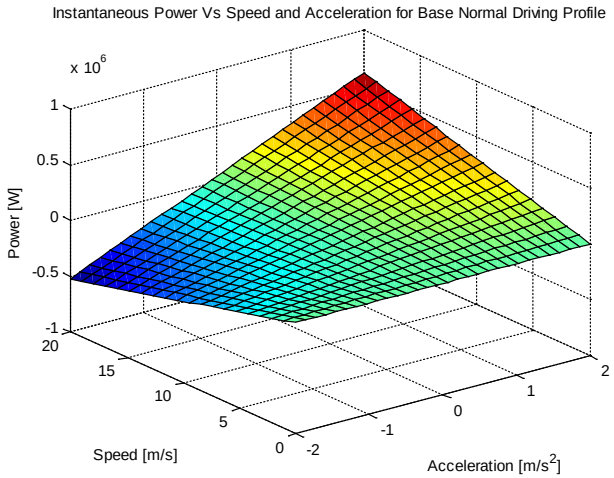

Fig. 27. Meta-model for the base normal driving profile

4.2.2 Optimization Problem

The main goal is to find an energy-optimal vehicle speed profile, i.e. a speed profile which reduces the total electric bus energy requirement for a particular route. To achieve it, the objective of the optimization problem is the minimization of the vehicle instantaneous power with respect to the acceleration. Since vehicle speed and acceleration are correlated, the optimal acceleration profile produces a new optimal velocity profile.

Because bus routes are tight to specific schedules that need to be met, the time is a critical factor. Thus, the optimization problem is subject to a constraint in time in order to try to keep the schedule within an acceptable range with respect to the original. Finally, a constraint in the optimal speed value is imposed in order to avoid the trivial solution.

The optimization problem is then formulated as in Equation (39).

$$\min_{a} f(v,a) = \min_{a}(\alpha_1 \cos(\theta)v + \alpha_2 \sin(\theta) + \alpha_3 va + \alpha_4 v^3) \tag{39}$$

$$\text{Subject to: } \begin{cases} t^* \le t_{ori}(1+q) \\ v_{lb} \le v^* \le v_{ub} \end{cases}$$

Where t^* is the total time for the optimal driving profile, t_{ori} is the total time for the original driving profile and q is a number between 0 and 1 defining the maximum allowed delay for the optimal total time with respect to the original, v^* is the optimal speed, and v_{lb}, v_{ub} are the lower and upper bounds for the vehicle speed.

4.2.3 Optimal velocity profile

The solution of the optimization is an energy-optimal acceleration profile which is used along with the data from the base normal driving profile to generate the final optimal speed profile.

In order to preserve the stops with respect to their original position and maintain the original distance of the route, the time intervals (Δt) are calculated from the original speed profile (v) and total distance (S) according to Equation (40).

$$S = \sum_{t=1}^{n+1} \Delta s_i = \sum_{k=0}^{n} (s_{k+1} - s_k)$$
$$S = \sum_{k=0}^{n} \left(v_k.(\Delta t) + \frac{1}{2}(v_{k+1} - v_k).(\Delta t) \right) \quad (40)$$

Then, the optimal speed profile is calculated at each instant of time using Equation (41).

$$v_{k+1}^{*} = v_k^{*} + a_k^{*}.(t_{k+1} - t_k) \quad (41)$$

4.2.4 Results

Three speed profiles were optimized and the potential energy savings were calculated for each case assuming that the optimal speed profile is followed with a 100% accuracy.

As a first approximation, an ideal speed profile, i.e., a trapezoid-shaped with symmetric acceleration and deceleration patterns (Fig. 28), was created by using information from Google Transit [105]. A route schedule for the Clemson Area Transit - CAT Bus, was utilized as base to generate an ideal speed profile schedule. The short 23 km speed profile was determined by assuming absence of traffic.

The remaining two speed profiles were generated from the ideal route schedule described in section 4.2.1. The route schedule was driven twice, one time using a normal driving style (Fig. 29) and a second time using a more aggressive driving style (Fig. 30). The difference between the two profiles can be confirmed by comparing the maximum acceleration values which remain higher for the aggressive drive.

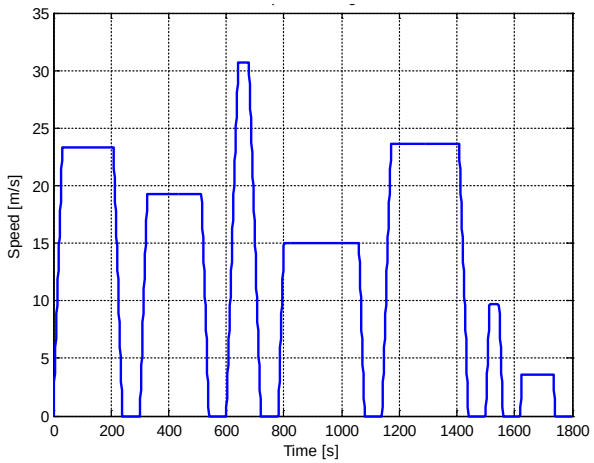

Fig. 28. Ideal speed profile – google transit

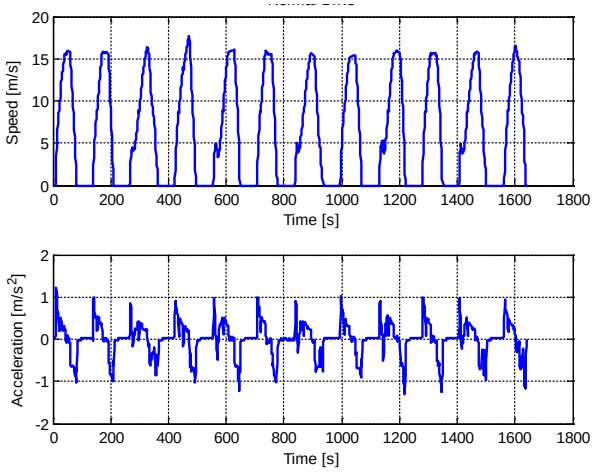

Fig. 29. Vehicle speed and acceleration profiles for normal drive

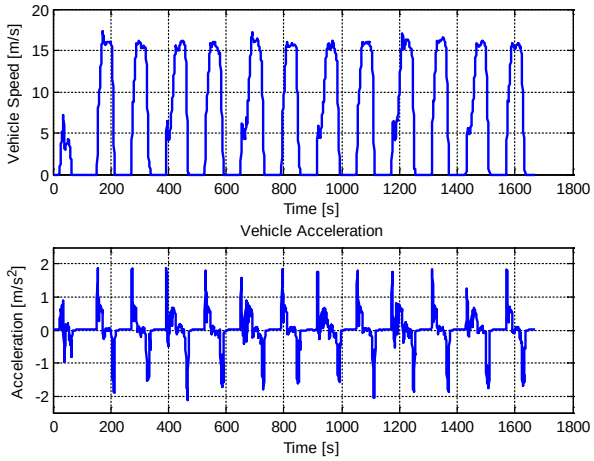

Fig. 30. Vehicle speed and acceleration profiles for aggressive drive

4.2.4.1 Google Transit

As seen in Fig. 31, an energy-optimal speed profile was obtained for the speed profile generated from google transit information. For this case, it is allowed a maximum delay of 10% over the base speed profile arrival time.

The optimized speed profile follows the constraint related to the position of the stops and describes a smooth acceleration and fast deceleration profiles. This goes along with the fact that faster deceleration will encourage a bigger regeneration portion while smoother acceleration will promote energy savings. Note that for the segments of the speed profile in which there are hard acceleration/deceleration patterns and short time at constant speed, the optimal speed profile reaches a lower maximum speed value compared to the base speed profile. As a consequence, the maximum acceleration value is also reduced. On the contrary, when acceleration/deceleration patterns are smoother, the optimal speed profile reaches higher maximum speed values. This allows compensating for the longer time accelerating at a lower rate in such a way that the maximum allowed time to reach the destination can be kept.

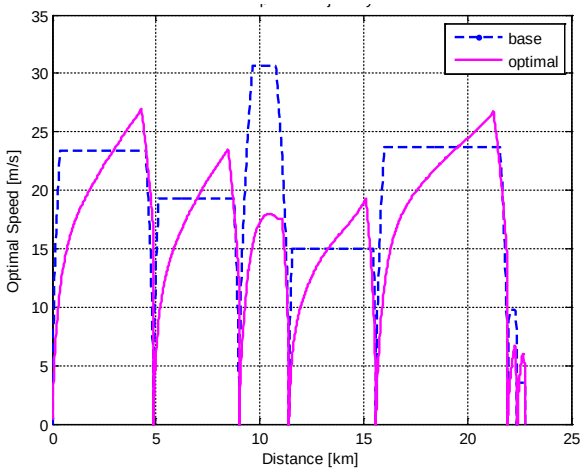

Fig. 31. Energy-Optimal speed profile vs distance for ideal speed profile – google transit

Fig. 32 shows that the optimal speed profile takes longer time to reach the destination than the base speed profile but remains inside the allowed 10%. In Fig. 33, the energy use for the optimal speed profile remains below the energy use for the base ideal driving profile. The total improvement is 5.3% which demonstrates the potential energy savings that can be achieved by using the proposed eco-driving tool.

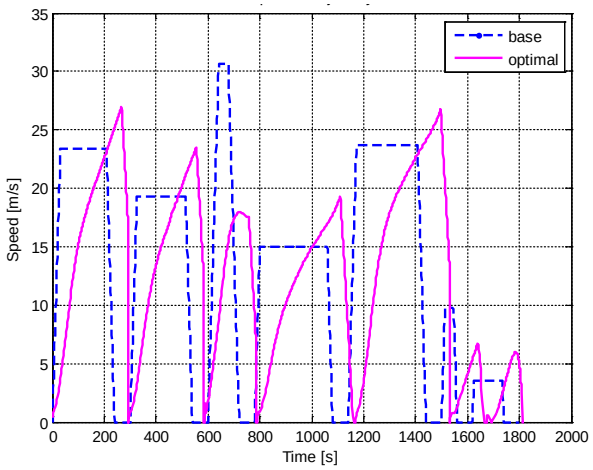

Fig. 32. Energy-Optimal speed profile vs time for ideal speed profile – google transit

4.2.4.2 Experimental Routes

According to the plots in Fig. 34 and Fig. 35, for the aggressive speed profile, the optimal speed remains below the speed values for the base case. Once again, to compensate for the lower speed values and remain in the allowed arrival time, the time spent at the bus stops is reduced. In this case, the arrival time is delayed by 0.7% of the baseline time.

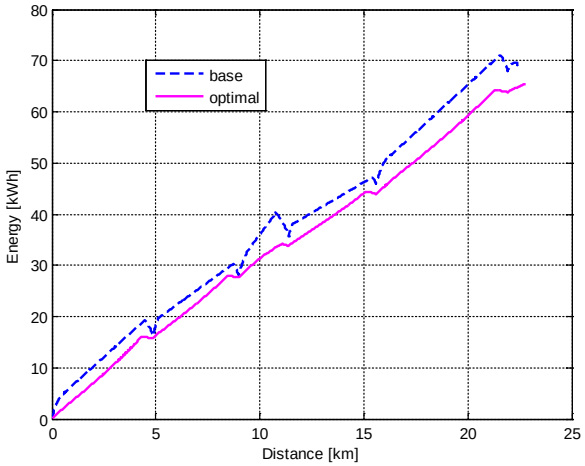

Fig. 33. Energy use for base and optimal speed profiles – ideal speed profile – Google Transit

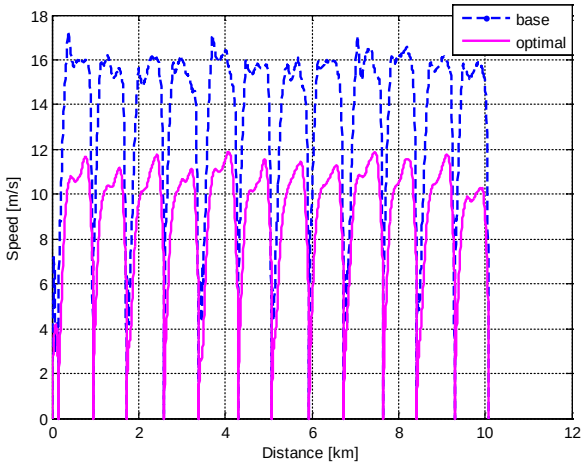

Fig. 34. Energy-Optimal speed profile vs distance for aggressive driving style

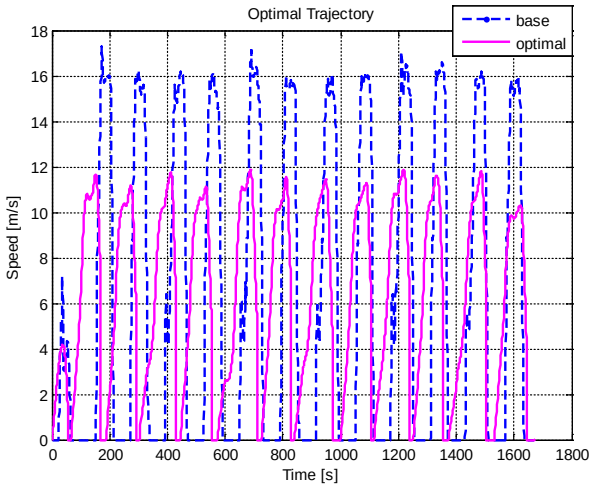

Fig. 35. Energy-Optimal speed profile vs time for aggressive driving style

Fig. 36 represents the energy use for the base and the optimized driving profiles. For the aggressive style, the achieved reduction was about 30.33%, which support the potential energy savings related to the use of the proposed eco-driving system. The optimization algorithm was also tested for the normal drive speed profile in Fig. 29. Vehicle speed and acceleration profiles for normal drive. The total energy used for this case was 19.47% less than for the base driving profile while the final arrival time was 6.3% shorter.

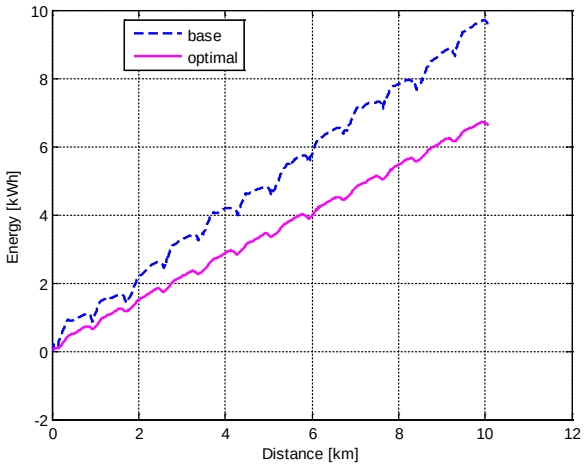

Fig. 36. Energy use for base and optimal speed profiles – normal style driving

4.2.5 Concluding remarks

The implemented eco-driving system optimizes a particular route schedule to minimize the bus energy consumption with a constraint on time. It provides online feedback and an offline score to the driver which allows comparing different drivers to a "theoretical optimal driver".

To test the performance of the system three different speed profiles were used and the corresponding energy-optimal speed profiles were generated. Assuming the driver

was able to closely follow the optimal speed profiles, it was estimated that the use of the system can yield energy consumption reductions of up to 30.33%.

CHAPTER FIVE

5 OPTIMAL TRAFFIC CONTROL AT MERGING HIGHWAYS[3]

The increasing demand for travel has generated significant challenges related to traffic congestion and accidents. Although driver responses to various disturbances can cause congestion [40], intersections and merging roadways are the primary sources of bottlenecks, further contributing to traffic congestion, which worsens at peak hours and accounts for additional fuel consumption [106]. In the United States, on average 5.5 billion hours are wasted each year due to vehicular congestion, which translates to about $121 billion dollars [1]. Moreover, the reduced speed imposed by traffic congestion can produce driver discomfort, distraction, and frustration, which may encourage more aggressive driving behavior [39] and further slow the process of recovering free traffic flow [2]. Safety and environmental issues are also attributed to vehicular traffic. In 2012, more than 2 million nonfatal injuries and 35,000 deaths were attributed to motor vehicles, and around 1.7 billion metric tons of CO2 were released to the environment by motor vehicles [1].

A significant research effort has been expended on improving traffic flow at intersections using connected vehicle technologies. Although heuristic approaches have been popular partly due to practical implications for online implementation, several optimization-based approaches have been proposed in the literature. This research work

[3] This work was supported by the Laboratory Directed Research and Development Program of the Oak Ridge National Laboratory, Oak Ridge, TN 37831 USA, managed by UT-Battelle, LLC, for the US Department of Energy (DOE), and in part by UT-Battelle, LLC, through DOE contract DE-AC05-00OR22725.

is concerned with improvement of the overall traffic efficiency on a portion of two convergent roads, which is similar to an intersection problem.

Although previous research reported in the literature has aimed at enhancing the understanding of coordinating vehicles at either intersections or merging roads, deriving an optimal closed-form solution in terms of fuel consumption that can be implemented online still remains a challenging control problem. Two main objectives here are: (1) to formulate the problem of optimal coordination of vehicles at merging roads under the hard constraint of collision avoidance and (2) to derive a closed-form solution that can be implemented online in a centralized fashion.

5.1 Problem formulation

Fig. 37 illustrates a common scenario in which a secondary one-lane road merges onto a main two-lane road. Typically, the vehicles on the secondary road have to yield to the vehicles on the main road and wait until the safest opportunity to merge onto the main road. On highly congested roads the merging process is even more tedious and undesired stop-and-go traffic flow becomes unavoidable. In this paper, we seek to improve the overall traffic efficiency in terms of fuel consumption on a portion of two convergent roads while indirectly improving travel time.

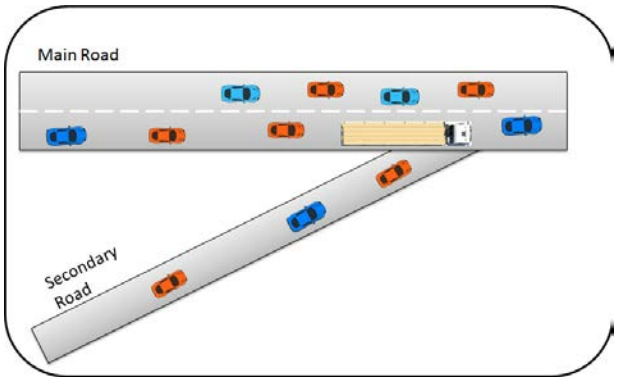

Fig. 37. Merging roads—scenario under consideration.

5.1.1 Notation

In our analysis, the subscript j denotes the road ($j=1$ for main road and $j=2$ for secondary road), the subscript i denotes each vehicle on the road, and the superscripts *0* and *f* denote the initial and final conditions. The variable u represents the control input, which in our case corresponds to the acceleration. The total number of merging roads/lanes is denoted by m, and the total number of vehicles on each road is denoted by n.

5.1.2 Modeling Framework

Each vehicle is subject to a second order dynamics, as defined by:

$$\begin{aligned} \dot{x}_i &= v_i \\ \dot{v}_i &= u_i, \end{aligned} \tag{42}$$

where x_i is the vehicle's i position $[m]$, v_i $[m/s]$ is the vehicle's i speed, and u_i is the vehicle's i acceleration (control input).

We consider a main and a secondary road merging together (Fig. 38). A centralized controller derives the optimal control policy (acceleration profile) in terms of fuel consumption for each vehicle driving inside a particular radius—defined as the control zone — under the hard constraint to enable the vehicles to cross the merging zone without collision.

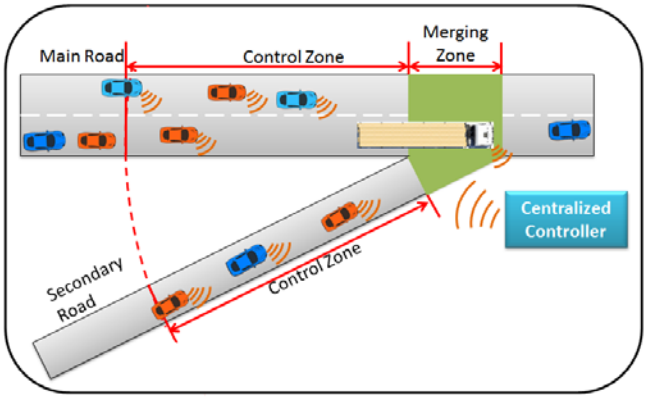

Fig. 38. Merging roads with connected vehicles.

It is assumed that each vehicle can communicate with the centralized controller. The vehicles transmit information regarding their locations and distances from the merging zone. Based on this information, the controller assigns a hierarchy to the vehicles and calculates the optimal control policy (acceleration profile) as a function of time for all vehicles in the control zone. The main goal is to reduce fuel consumption while coordinating the vehicles crossing the merging zone by achieving a continuous traffic flow. The optimal control policy of the centralized controller for each vehicle is communicated to the corresponding vehicle. If the vehicles are autonomous, then they will just follow the policy imposed by the controller. If there is a driver, then the implicit assumption is that the driver will follow the control policy—provided as instructions—of

the centralized controller. Future research should investigate how to incentivize, or persuade, drivers to follow the instructions.

It is wanted to reduce fuel consumption by minimizing the acceleration while improving the traffic flow on a merging point of two roads by coordinating the vehicles inside a control zone (Fig. 39).

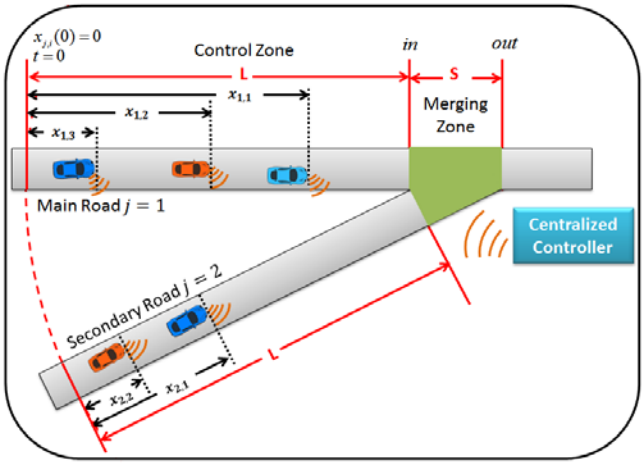

Fig. 39. Simplified scenario: two one-lane merging roads.

To estimate the fuel consumption, we use the polynomial meta-model proposed in [107] that yields vehicle fuel consumption as a function of the speed and acceleration:

$$f_v = f_{cruise} + f_{accel}, \tag{43}$$

where $f_{cruise} = w_0 + w_1 \cdot v + w_2 \cdot v^2 + w_3 \cdot v^3$ estimates the fuel consumed by a vehicle traveling at a constant speed v, and $f_{accel} = a \cdot (r_0 + r_1 \cdot v + r_2 \cdot v^2)$ is the additional fuel consumption caused by acceleration. The polynomial coefficients w_i and r_i are calculated from experimental data. For the vehicle parameters reported in [107], where the vehicle mass is $M_v = 1,200$ kg, the drag coefficient is $C_D = 0.32$, the air density is

$\rho_a = 1.184$ km/m3, the frontal area is $A_f = 2.5$ m2, and the rolling resistance coefficient is $\mu = 0.015$, the polynomial coefficients are: $w_0 = 0.1569$, $w_1 = 2.45 \times 10^{-2}$, $w_2 = -7.415 \times 10^{-4}$, $w_3 = 5.975 \times 10^{-5}$, $r_0 = 0.07224$, $r_1 = 9.681 \times 10^{-2}$, and $r_2 = 1.075 \times 10^{-3}$.

5.1.3 Optimization Problem Formulation

Fig. 40 illustrates the fuel consumption variation with respect to the vehicle speed and acceleration. Clearly, there is a monotonic relationship between fuel consumption and acceleration. Consequently, instead of formulating a fuel consumption minimization problem we can formulate the problem considering vehicle acceleration which result in reduced fuel consumption. In this context, the objective is to find for each vehicle the optimal acceleration profile from the time they enter in the control zone until the time they exit the merging zone.

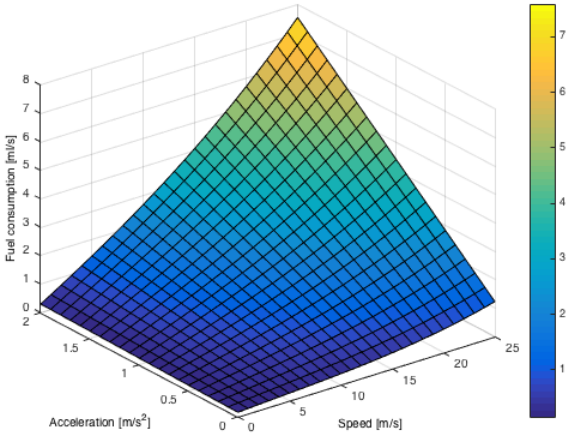

Fig. 40. Fuel consumption model.

The initial and final conditions are related to each vehicle's position and speed. More specifically, the initial position for vehicle *i* in the road *j* refers to the starting point of the control zone, $x_{j,i}(t_{j,i}^0)$; similarly, the initial condition for the speed is the one that the vehicle has when entering the control zone, $v_{j,i}(t_{j,i}^0)$, i.e., the driver's desired speed, v_{des}, which the vehicle has when it enters the control zone. Similarly, the final condition for control is the position at which the vehicle leaves the merging zone, $x_{j,i}(t_{j,i}^f)$. We assume that after leaving the merging zone the driver would wish to return back to the initial desired speed, v_{des}.

To ensure the absence of collisions, we consider the following constraints in our problem formulation. To avoid rear end collisions for vehicles on the same roads, we impose the condition that the position of the precedent vehicle, $x_{j,i}(t)$, should be greater than or equal to the position of the following vehicle, $x_{j,i+1}(t)$, plus a predefined safe distance δ. To avoid lateral collisions when the vehicles from the secondary road are merging into the primary road, we impose the condition that the vehicles are going to be coordinated on a first come, first serve basis.

To simplify notation, we make an explicit distinction between the vehicles traveling on the primary road, i.e., we will use $j=1$, and those traveling on the secondary road, i.e., we will use $j=2$. Thus, if the difference between the position of the vehicle *i* traveling on the primary road, $x_{1,i}(t)$, and the position of a vehicle *k* traveling on the secondary road, $x_{2,k}(t)$, is less than the length of the merging zone, S, then, the

vehicle which is closer to the merging zone will be served first. For example, if at time *t* the position of the vehicle on the primary road, $x_{1,i}(t)$, is greater than the position of the vehicle on the secondary road, $x_{2,k}(t)$, the vehicle on the primary road is closer to the merging zone and will be served first. Consequently, the vehicle in the secondary road will be controlled in such a way that it will reach the merging zone only by the time the vehicle $x_{1,i}(t)$ has exited it.

The optimization problem is formulated as follows:

$$\min_{u_{j,i}} J = \min_{u_{j,i}} \frac{1}{2} \sum_{j=1}^{2} \sum_{i=1}^{n} \int_0^{t_{j,i}^{out}} {u_{j,i}}^2 dt \,, \tag{44}$$

Subject to

- Vehicle dynamics:

$$\dot{x}_{j,i} = v_{j,i}$$
$$\dot{v}_{j,i} = u_{j,i}$$

- Initial conditions:

$$x_{j,i}(t_{j,i}^0) = 0$$
$$v_{j,i}(t_{j,i}^0) = v_{j,i}(t)$$

- Final conditions:

$$x_{j,i}(t_{j,i}^f) = L + S - x_{j,i}(t)$$
$$v_{j,i}(t_{j,i}^f) = v_{des}$$

- Safety constraints:
    - Rear end collision avoidance:

$$x_{j,i}(t) \geq x_{j,i+1}(t) + \delta$$

- Lateral collision avoidance:

  If $\left|x_{1,i}(t) - x_{2,k}(t)\right| \le S$,

  Then

  $$\text{If } x_{1,i}(t) \ge x_{2,k}(t) \Rightarrow x_{2,k}(t_{2,k}^f) \le x_{1,i}(t_{1,i}^f) - S$$

  $$\text{else } x_{1,i}(t_{1,i}^f) \le x_{2,k}(t_{2,k}^f) - S \text{ .}$$

The analytical solution to this optimization problem is presented next.

5.2 Analytical solution

To address this problem we consider the following three steps: (1) defining a hierarchical vehicle sequence based on which vehicle is closer to the merging zone, (2) assigning the times for each vehicle to reach and leave the merging zone that guarantee collision avoidance, and (3) finding the closed-form analytical solution for the optimization problem.

5.2.1 Defining the hierarchical vehicle sequence

When a vehicle reaches the control zone it starts communicating its position to the centralized controller. Then the controller defines a hierarchical vehicle sequence starting with the vehicle that is closer to the merging zone (Fig. 41). If two vehicles on different roads have the same distance from the merging zone, the priority will be given to the vehicle on the main road. Note that with such a hierarchy, the problem of blocked lanes is

avoided because, at each instant of time, only the vehicle that is closest to the merging zone will have the right-of-way.

In our analysis, we use a single subscript identifying each vehicle on the control zone, starting from the one that is closest to the merging zone, i.e., $i=1$, to the one which is farthest from the merging zone.

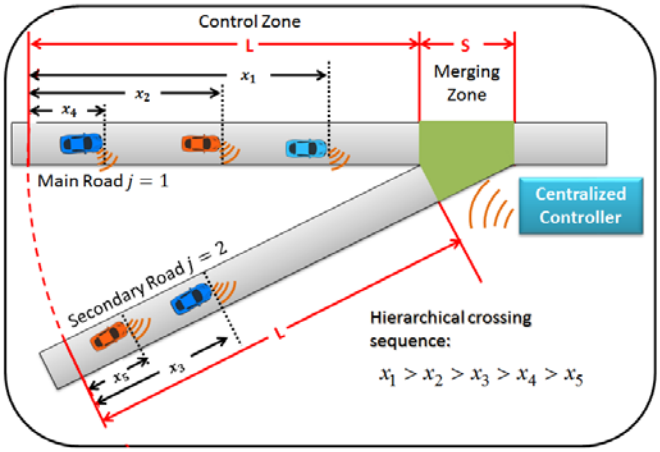

Fig. 41. Hierarchical crossing sequence.

5.2.2 Assigning the times to enter and exit the merging zone

Once the hierarchy is defined, the controller assigns to each vehicle *i* in the control zone the time, t_i^{in}, to enter the merging zone. To eliminate the chance of lateral collisions we impose the condition that only one vehicle at a time can be in the merging zone. Thus, the time for each vehicle *i*, t_i^{in}, to enter the merging zone is determined by the time, t_{i-1}^{out}, that the previous vehicle, *i-1*, in the hierarchy has exited it, as illustrated in Fig. 42.

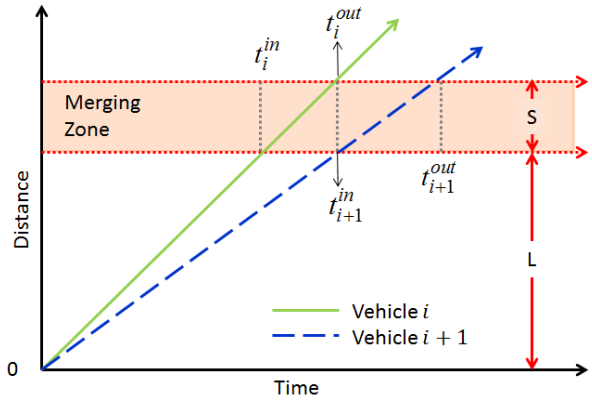

Fig. 42. Illustration of time calculation for vehicles entering the merging zone from different roads.

For vehicles traveling on the same road, this constraint is modified to maintain a minimum safe distance, δ, between them, as shown in Fig. 43.

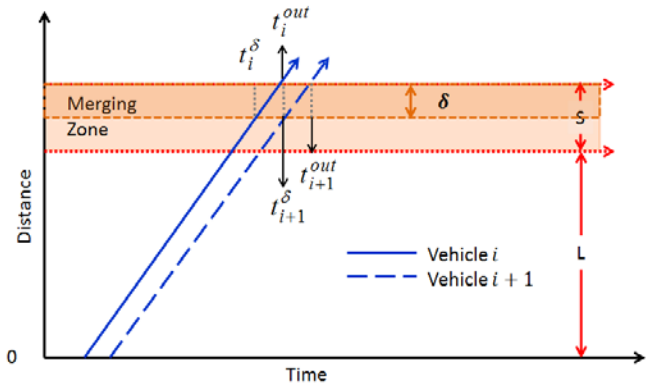

Fig. 43. Illustration of time calculation for vehicles entering the merging zone on the same road.

These times, which impose the constraints to avoid either lateral or rear end collisions, are assigned at each instant of time to allow readjustment according to the traffic conditions.

Based on the previous two steps, the optimal control problem for *n* vehicles is formulated as follows

$$\min_{u_i} J = \min_{u_i} \frac{1}{2} \sum_{i=1}^{n} \int_0^{t_i^f} u_i^2 dt \tag{45}$$

Subject to

- Vehicle dynamics:

$$\dot{x}_i = v_i$$
$$\dot{v}_i = u_i$$

- Initial conditions:

$$x_i(t_i^0) = 0$$
$$v_i(t_i^0) = v_i(t)$$

- Final conditions:

$$x_i(t_i^f) = L + S - x_i(t)$$
$$v_i(t_i^f) = v_{des}$$

- Safety constraints:
    - Rear end collisions avoidance:

$$t_{i+1}^{\delta} \geq t_i^{out}$$

    - Lateral collisions avoidance:

$$t_{i+1}^{in} \geq t_i^{out}$$

where t_i^0 is the time that the vehicle *i* enters the control zone, and t_i^f is the time the vehicle *i* exits the merging zone. Thus, the safety constraints have been translated into time constraints and will be used with the boundary conditions for the analytical solution. Since the initial vehicle speed when the vehicle enters the control zone is the driver's desired speed, we designate the final speed, when the vehicle exits the merging zone to be equal to the initial speed. However, this could be modified appropriately.

5.2.3 Analytical solution

For the analytical solution of problem (3), Pontryagin's minimum principle is applied. We seek to find the optimal control $u^*(t)$ which drives the system along an optimal trajectory $x^*(t)$. For each vehicle *i*, the Hamiltonian function of the above optimization problem is

$$H_i(\lambda_i^x, \lambda_i^v, x_i, v_i) = \frac{1}{2}u_i^2 + \lambda_i^x v_i + \lambda_i^v u_i \tag{46}$$

where λ_i^v and λ_i^u are the co-state components. Applying the Hamiltonian minimization condition, the optimal control can be given as a function of the co-states

$$u_i^* + \lambda_i^v = 0. \tag{47}$$

The adjoin equations yield

$$\dot{\lambda}_i^x = -\frac{\partial H}{\partial x_i} = 0 \tag{48}$$

$$\dot{\lambda}_i^v = -\frac{\partial H}{\partial v_i} = -\lambda_i^x, \tag{49}$$

and hence $u_i^* = -\lambda_i^v$. From (48) we have $\lambda_i^x = a_i$ and from (49) implies $\lambda_i^v = -(a_i t + b_i)$, where a_i and b_i are constants of integration corresponding to each vehicle *i*. Consequently, the optimal control input (acceleration/deceleration profile) as a function of time is given by

$$u_i^* = a_i t + b_i. \tag{50}$$

Substituting the last equation to the vehicle dynamics equations (1) we can find the optimal speed and position for each vehicle, namely

$$v_i^*(t) = \frac{1}{2}a_i t^2 + b_i t + c_i \tag{51}$$

$$x_i^*(t) = \frac{1}{6}a_i t^3 + \frac{1}{2}b_i t^2 + c_i t + d_i, \tag{52}$$

where c_i and d_i are constants of integration. The constants a_i, b_i, c_i, and d_i can be computed by the initial and final conditions in (53). It is important to emphasize that this analytical solution can be implemented online. To derive online the optimal control for each vehicle, we need to update the integration constants at each time *t*. Equations (51) and (52) along with the initial and final conditions defined in the optimization problem (45) can be used to form a system of four equations of the form $\mathbf{T_i b_i = q_i}$. Note that in this step, we are already satisfying the initial and final conditions, including the safety constraints.

$$\begin{bmatrix} \frac{1}{6}(t_i^0)^3 & \frac{1}{2}(t_i^0)^2 & t_i^0 & 1 \\ \frac{1}{2}(t_i^0)^2 & t_i^0 & 1 & 0 \\ \frac{1}{6}(t_i^f)^3 & \frac{1}{2}(t_i^f)^2 & t_i^f & 1 \\ \frac{1}{2}(t_i^f)^2 & t_i^f & 1 & 0 \end{bmatrix} \cdot \begin{bmatrix} a_i \\ b_i \\ c_i \\ d_i \end{bmatrix} = \begin{bmatrix} x_i(t_i^0) \\ v_i(t_i^0) \\ x_i(t_i^f) \\ v_i(t_i^f) \end{bmatrix} \tag{53}$$

Hence we have

$$\mathbf{b_i} = (\mathbf{T_i})^{-1} \cdot \mathbf{q_i} \tag{54}$$

where $\mathbf{b_i}$ is a vector containing the four integration constants a_i, b_i, c_i and d_i. As we continuously update the constants using (53) the controller yields the closed-loop optimal acceleration/deceleration for each vehicle *i* over time from (50), .

5.3 Simulation Results

To validate the effectiveness of the efficiency of our analytical solution we simulated the merging scenario presented in previous section in Matlab/Simulink. In our case study, the length of the control zone is 400 m, and the merging zone length is 30 m. It is assumed that each vehicle travels at a constant speed of 30 mph (13.41 m/s) before entering the control zone. As soon as a vehicle reaches the control zone then the centralized controller designates the acceleration/deceleration profile for each vehicle until it exits the merging zone. All vehicles are assumed to have the characteristics described in Section II.

We considered the case of coordinating 30 vehicles, 15 for each road. The centralized controller is able to derive online the optimal control (acceleration/deceleration profile) by avoiding collision in the merging zone, while only one vehicle at the time was crossing the merging zone, as illustrated in Fig. 44.

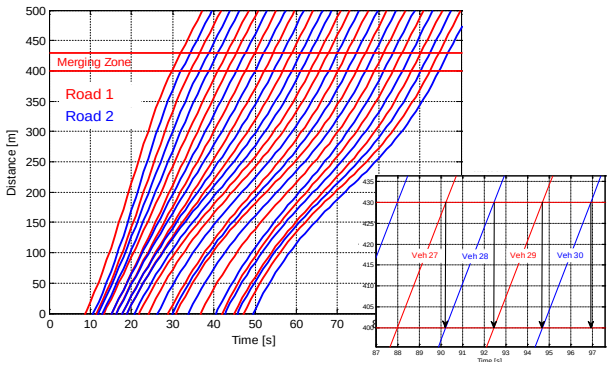

Fig. 44. Distance of the thirty vehicles traveled in merging coordination (road 1 corresponds to the main road and road 2 corresponds to the secondary road).

We note that as the number of vehicles on each road in the control zone increases, there is an impact on the acceleration profile for each vehicle (Fig. 45). The controller

accelerates the vehicles that are closer to the merging zone to create more space in the road for the vehicles following. However, as the number of vehicles on the road increases and reaches its maximum capacity, eventually the vehicles entering the control zone need to decelerate (Fig. 45).

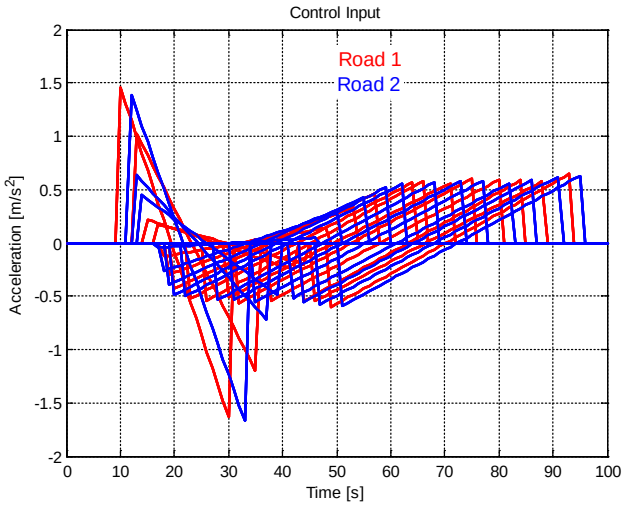

Fig. 45. Acceleration profile in merging coordination of thirty vehicles (road 1 corresponds to the main road and road 2 corresponds to the secondary road).

As a result, the vehicles ahead in the hierarchy are able to cross the control zone in a shorter time than the rest of the vehicles. Thus, as the number of vehicles increases, at some point of time the vehicles that enter the control zone may be required to come to a full stop as imposed by the road capacity constraints. Note that the little jumps above the desired speed in (Fig. 46) are due to the fact that the matrix *Ti* in (54) tends to become singular when the vehicle *i* exits the merging zone.

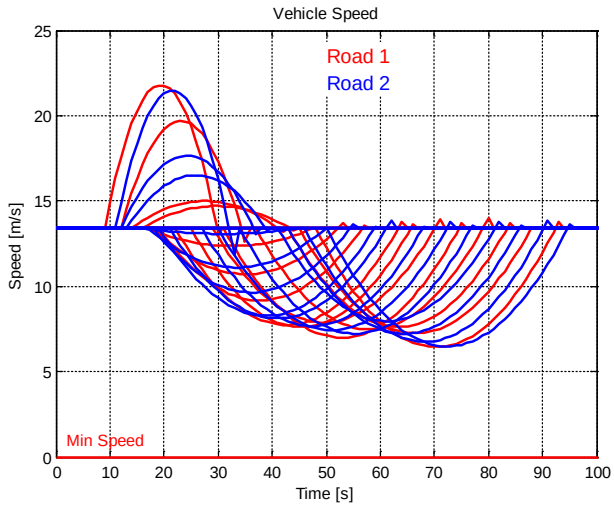

Fig. 46. Speed profile in merging coordination of thirty vehicles (road 1 corresponds to the main road and road 2 corresponds to the secondary road).

The optimal solution for the vehicle coordination was compared to a baseline scenario. In the baseline scenario, the vehicles on the main road have the right-of-way, so all the vehicles in the secondary road need to come to a full stop before they enter the merging zone and wait until the vehicles on the main road cross the merging zone. That is, the vehicles on the secondary road have to come to a full stop before entering the merging zone. The optimal acceleration/deceleration profile imposed by the controller resulted in minimizing fuel consumption both at the control zone and merging zone as shown in Fig. 47. The fuel consumption improvement in the coordinated scenario is due to the fact that the vehicles coming from the secondary road do not come to a full stop before they enter to the main road, thereby conserving momentum and fuel while also improving travel time.

5.3.1 Fuel consumption results for a fleet of 30 conventional vehicles

The overall fuel consumption improvement when the conventional vehicles are coordinated compared to the baseline scenario is 49.8%. Moreover, the coordination of vehicles resulted in improving the total travel time by 6.9% compared to the baseline (Fig. 48).

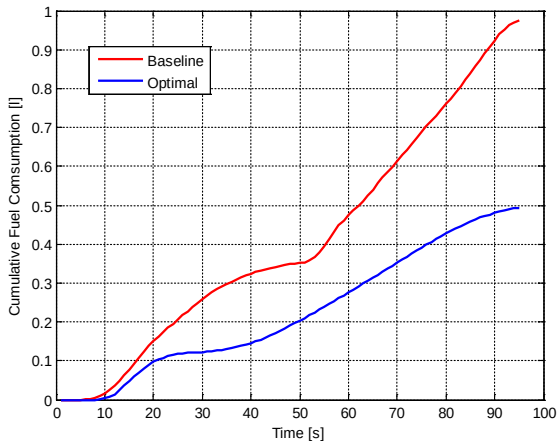

Fig. 47. Cumulative fuel consumption comparison.

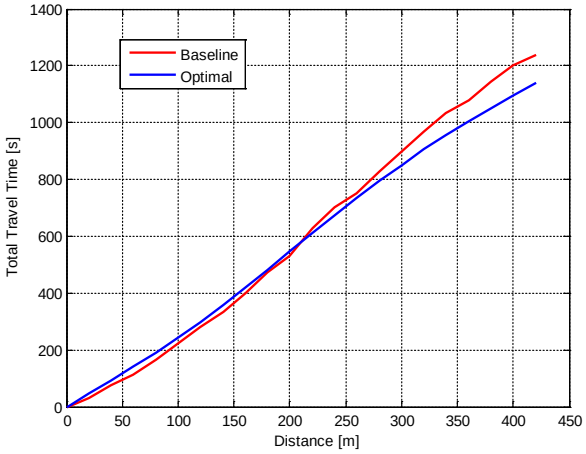

Fig. 48. Total travel time.

5.3.2 Fuel consumption results for a fleet of 30 HEVs

To evaluate the benefits of integrating Hybrid Electric Vehicles and the coordination algorithm, the baseline and the optimized driving profiles obtained with the simulations, were used to run the simulator described in section 3.3.1, which corresponds to a parallel through the road powertrain configuration, using the ECMS as the energy management strategy.

The overall fuel consumption improvement when the 30 HEVs are coordinated compared to the baseline scenario (also with HEVs) is 47%. The slightly decreased result is due to the fact that HEVs can perform better than conventional engine-powered vehicles in stop and go operation.

5.4 Concluding remarks

An analytical formulation for the problem of optimally coordinating the trajectories of vehicles traveling over two merging highways was developed. The problem was translated into a constrained optimization problem that aims to find a safe and fuel-efficient crossing schedule, i.e., velocity profile and arrival time to the merging zone, for all the vehicles in a control zone. Fuel-efficiency is indirectly addressed by using acceleration as the objective function of the optimal control problem. Then, by applying Pontryagin's minimum principle, it was showed that it is possible to obtain a closed-form solution, which allows the implementation of a centralized real-time optimal control.

The effectiveness of the control policies was validated through simulations, which showed the system outperformed a baseline scenario where there was no coordination and the vehicles were required to stop

CHAPTER SIX

6 CONCLUSIONS AND FUTURE WORK

This dissertation work explores different methods for the optimization/reduction of the vehicle's energy/fuel utilization.

In chapter three, the research efforts are concentrated in the optimization of the fuel consumption for hybrid electric vehicles. In particular, the problem of finding more efficient techniques to tune the equivalent factor of the ECMS is addressed, and four different strategies are proposed. The first two strategies, based on model predictive control, allow updating of the *s* factor along a particular driving profile. In the first MPC-based approach, roadway traffic prediction data is sent to the supervisory controller to tune the ECMS algorithm for a particular time window length, resulting in reduction of up to 4.28% in fuel consumption. In the second MPC-based approach, the control input is periodically recalculated, allowing adaptation to changes in the initially predicted driving profile for the entire trip and fuel consumption reduction of up to 6.85%. The remaining two strategies, based on the analysis of the operating points distribution, involve the use of the Willans-line model to estimate the engine fuel consumption. Although the tuning of the equivalence factor *s* is still required, the use of the intrinsic efficiency and its stated relation to the equivalence factor, allows finding a probable range for it, speeding up the tuning process. Furthermore, the new operating point distribution, resulting from the use of the Willans-line model, is useful to facilitate the real-time tuning of the strategy. For the proposed numerical solutions, even though the results are slightly worse than for the case of the map-based ECMS strategy, it is found that the number of iterations required to

find an optimal sustaining value for *s*, can be reduced to 0.059% the number of iterations required with a standard iterative approach. This confirms their potential for real time implementation.

Then, in chapter four, the research is extended to the fuel/energy utilization optimization for conventional and electric vehicles, in which case the effects of having smoother driving profiles are explored. In this case, it is found that driving profile optimization and eco-driving can contribute with meaningful energy savings for conventional and electric vehicles. In the particular case of electric powertrains, and assuming the driver is able to closely follow the optimal speed profiles proposed by an eco-driving system, it is estimated that energy consumption reductions of up to 30.33% can be achieved.

Finally, in chapter five the research focus on vehicle coordination control at merging highways to avoid frequent acceleration/deceleration patterns for a fleet of vehicles. An analytical formulation for the problem of optimally coordinating the trajectories of vehicles traveling over two merging highways is developed. The problem is translated into a constrained optimization problem that aims to find a safe and fuel-efficient crossing schedule, i.e., velocity profile and arrival time to the merging zone, for all the vehicles in a control zone. Fuel-efficiency is indirectly addressed by using acceleration as the objective function of the optimal control problem. Then, by applying Pontryagin's minimum principle, it is shown that it is possible to obtain a closed-form solution, which allows the implementation of a centralized real-time optimal control. The effectiveness of the control policies is validated through simulations, showing that the

system outperformed a baseline scenario where there is not coordination and the vehicles are required to stop.

6.1 Future work

The present research work can be extended in different directions as suggested below.

For the case of the Willans-based tuning strategies, it is proposed as future work to consider the efficiencies of the electric motor, generator, etc., as well as the dependence of the engine's intrinsic efficiency on the torque. Such considerations, converts the problem into a 3D problem in which the regions illustrated in Fig. 16, are to be separated by a surface instead of a line.

For the case of the eco-driving system, there are still aspects to be improved to achieve more realistic outcomes:

- ✓ In the case of significant changes with respect to the base driving profile, the meta-model utilized to estimate the instantaneous power may not be accurate enough to represent the vehicle behavior. Thus, a new meta-model has to be recalculated for each new driving profile.
- ✓ As the problem is solved offline, the eco-driving system will not adapt to changing traffic conditions. Consequently, in case of significant changes in the base driving profile the optimality of the solution will not be valid and the percentage of improvement may be lower. Therefore, finding a solution which allows online implementation is a desired goal.

- ✓ Many other factors influencing the vehicle energy use are still to be studied. Analyses are to be done about how to integrate those in the optimization strategy. In particular, the analysis of the experimental information gathered during the execution of the project, allowed to identify the road grade, cornering effects and the wind speed as important factors influencing the vehicle energy consumption.

For the centralized traffic coordination system, it is proposed to explore the uncertainty produced in the system by having drivers who do not follow the given instructions. Additionally, the coordination of vehicles around roundabouts and the control on a road network containing interconnected merging/intersection points and roundabouts will extend and complement the results presented in this dissertation.

REFERENCES

[1] "U.S. Department of Transportation. 'National Transportation Statistics 2012,'" 2012.

[2] V. L. Knoop, H. J. Van Zuylen, and S. P. Hoogendoorn, "Microscopic Traffic Behaviour near Accidents," in *18th International Symposium of Transportation and Traffic Theory*, 2009.

[3] "U.S. Department of Energy, Oak Ridge National Laboratory, Transportation Energy Data Book, Edition 30," 2011.

[4] A. A. Malikopoulos, "Supervisory Power Management Control Algorithms for Hybrid Electric Vehicles: A Survey," *IEEE Trans. Intell. Transp. Syst.*, vol. 15, no. 5, pp. 1869–1885, 2014.

[5] F. R. Salmasi, "Control Strategies for Hybrid Electric Vehicles: Evolution, Classification, Comparison, and Future Trends," *IEEE Trans. Veh. Technol.*, vol. 56, no. 5, pp. 2393–2404, 2007.

[6] A. Sciarretta and L. Guzzella, "Control of Hybrid Electric Vehicles," *Control Syst.*, vol. 27, no. 2, pp. 60–70, 2007.

[7] A. Balazs, E. Morra, and S. Pischinger, "Optimization of Electrified Powertrains for City Cars," *SAE Int. J. Alt. Power.*, vol. 1, no. 2, pp. 381–394, 2012.

[8] A. R. Salisa, N. Zhang, and J. G. Zhu, "A Comparative Analysis of Fuel Economy and Emissions Between a Conventional HEV and the UTS PHEV," *IEEE Trans. Veh. Technol.*, vol. 60, no. 1, pp. 44–54, 2011.

[9] P. Pisu and G. Rizzoni, "A Comparative Study Of Supervisory Control Strategies for Hybrid Electric Vehicles," *IEEE Trans. Control Syst. Technol.*, vol. 13, no. 3, pp. 506–518, 2007.

[10] H. Banvait, S. Anwar, and C. Yaobin, "A rule-based energy management strategy for Plug-in Hybrid Electric Vehicle (PHEV)," in *American Control Conference*, 2009, pp. 3938–3943.

[11] A. Sciarretta, M. Back, and L. Guzzella, "Optimal Control of Parallel Hybrid Electric Vehicles," vol. 12, no. 3, pp. 352–363, 2004.

[12] C.-C. Lin, P. Huei, and J. W. Grizzle, “A stochastic control strategy for hybrid electric vehicles,” in *Proceedings of the American Control Conference*, 2004, pp. 4710 –4715.

[13] Y. Bin, Y. Li, Q. Gong, and Z.-R. Peng, “Multi-information integrated trip specific optimal power management for plug-in hybrid electric vehicles,” in *Procedings of the american control conference*, 2009, pp. 4607 – 4612.

[14] D. V. Ngo, T. Hofman, M. Steinbuch, and A. F. A. Serrarens, “An optimal control-based algorithm for Hybrid Electric Vehicle using preview route information,” in *Proceedings of the American Control Conference*, 2010, pp. 5818 – 5823.

[15] S. Stockar, V. Marano, M. Canova, G. Rizzoni, and L. Guzzella, “Energy-Optimal Control of Plug-in Hybrid Electric Vehicles for Real-World Driving Cycles,” *IEEE Trans. Veh. Technol.*, vol. 60, no. 7, pp. 2949 – 2962, 2011.

[16] L. Serrao, S. Onori, and G. Rizzoni, “A comparative analysis of energy management strategies for Hybrid Electric Vehicles,” *J. Dyn. Syst. Meas. Control*, vol. 133, no. 3, 2011.

[17] N. Kim, S. Cha, and H. Peng, “Optimal Control of Hybrid Electric Vehicles Based on Pontryagin’s Minimum Principle,” *IEEE Trans. Control Syst. Technol.*, vol. 19, no. 5, pp. 1279 – 1287, 2011.

[18] P. Pisu, K. Koprubasi, and G. Rizzoni, “Energy Management and Drivability Control Problems for Hybrid Electric Vehicles,” in *Procedings of the IEEE Conference in Decision and Control*, 2005, pp. 1824 – 1830.

[19] P. Pisu and G. Rizzoni, “A supervisory control strategy for series hybrid electric vehicles with two energy storage systems,” in *Proceedings of the IEEE Conference on Vehicle Power and Propulsion*, 2005.

[20] S. Onori, L. Serrao, and G. Rizzoni, “Adaptive Equivalent Consumption Minimization Strategy for Hybrid Electric Vehicles,” in *Proceedings of the 2010 Asme Conference*, 2010.

[21] C. Zhang and A. Vahidi, “Real-time optimal control of plug-in hybrid vehicles with trip preview,” in *Proceedigs of the 2010 American Control Conference*, 2010, p. 6917,6922.

[22] L. Serrao, S. Onori, and G. Rizzoni, “ECMS as a realization of Pontryagin’s minimum principle for HEV control,” in *Proceedings of the American Control Conference*, 2009, pp. 3964 – 3969.

[23] P. Pisu, K. Koprubasi, and G. Rizzoni, “Energy Management and Drivability Control Problems for Hybrid Electric Vehicles,” in *44th IEEE Conference on Decision and Control and 2005 European Control Conference*, 2005, p. 1824,1830.

[24] J. Rios and P. Pisu, “A Comparative Analysis of Optimization Strategies for a Power-Split Powertrain Hybrid Electric Vehicle,” in *Proceedings of the FISITA 2012 World Automotive Congress, Springer Berling Heidelberg*, 2012, pp. 541–550.

[25] S. Onori and L. Serrao, “On Adaptive-ECMS strategies for hybrid electric vehicles,” in *2nd International scientific conference on hybrid and electric vehicles RHEVE*, 2011.

[26] F. Lacandia, L. Tribioli, S. Onori, and G. Rizzoni, “Adaptive Energy Management Strategy Calibration in PHEVs Based on a Sensitivity Study,” *SAE Int. J. Alt. Power*, vol. 2, no. 3, pp. 443–455, 2013.

[27] A. Asadi, B., Zhang, C., and Vahidi, “The role of traffic flow preview for planning fuel optimal vehicle velocity,” in *ASME Dynamic Systems and Control Conference*, 2010, pp. 1–7.

[28] B. Asadi and A. Vahidi, “Predictive cruise control: Utilizing upcoming traffic signal information for improving fuel economy and reducing trip time,” *IEEE Trans. Control Syst. Technol.*, vol. 19, no. 3, pp. 707–714, 2011.

[29] M. A. S. Kamal, M. Mukai, J. Murata, and T. Kawabe, “On board eco-driving system for varying road-traffic environments using model predictive control,” in *Proceedings of the 2010 IEEE International Conference in Control Applications*, 2010, pp. 1636–1641.

[30] M. a. S. Kamal, M. Mukai, J. Murata, and T. Kawabe, “Ecological Vehicle Control on Roads With Up-Down Slopes,” *IEEE Trans. Intell. Transp. Syst.*, vol. 12, no. 3, pp. 783–794, Sep. 2011.

[31] “AIMSUN, Traffic Modeling Software.” [Online]. Available: http://www.aimsun.com.

[32] A. S. Kamal, J. Imura, T. Hayakawa, A. Ohata, and K. Aihara, “Smart Driving of a Vehicle Using Model Predictive Control for Improving Traffic Flow,” *IEEE Trans. Intell. Transp. Syst.*, vol. 15, no. 2, pp. 878–888, 2014.

[33] C. Zhang and A. Vahidi, “Predictive Cruise Control With Probabilistic Constraints for Eco Driving,” in *ASME 2011 Dynamic Systems and Control Conference*, 2011, pp. 1–6.

[34] M. Kerper, C. Wewetzer, H. Trompeter, W. Kiess, and M. Mauve, “Driving More Efficiently - The Use of Inter-Vehicle Communication to Predict a Future Velocity Profile,” in *Proceedings of the 2011 IEEE 73rd Vehicular Technology Conference (VTC Spring)*, 2011, pp. 1–5.

[35] F. Mensing, R. Trigui, and E. Bideaux, “Vehicle trajectory optimization for application in ECO-driving,” in *Proceedings of the 2011 IEEE Vehicle Power and Propulsion Conference (VPPC)*, 2011, pp. 1–6.

[36] J. Wollaeger, S. A. Kumar, S. Onori, D. Filev, Ü. Özgüner, G. Rizzoni, and S. Di Cairano, “Cloud - computing based Velocity Profile Generation for Minimum Fuel Consumption : A Dynamic Programming based Solution,” in *Proceedings of the 2012 American Control Conference*, 2012, pp. 2108–2113.

[37] Y. Chen, D. Zhang, and K. Li, “Enhanced eco-driving system based on V2X communication,” in *Proceedings of the 2012 15th International IEEE Conference on Intelligent Transportation Systems*, 2012, pp. 200–205.

[38] X. Ma, “Towards intelligent fleet management: Local optimal speeds for fuel and emissions,” *16th Int. IEEE Conf. Intell. Transp. Syst. (ITSC 2013)*, pp. 2201–2206, Oct. 2013.

[39] A. A. Malikopoulos and J. P. Aguilar, “Optimization of driving styles for fuel economy improvement,” in *Proceedings of the 2012 15th International IEEE Conference on Intelligent Transportation Systems*, 2012, p. 194,199.

[40] A. A. Malikopoulos and J. P. Aguilar, “An Optimization Framework for Driver Feedback Systems,” *IEEE Trans. Intell. Transp. Syst.*, vol. 14, no. 2, pp. 955–964, 2013.

[41] Q. Cheng, L. Nouveliere, and O. Orfila, “A new eco-driving assistance system for a light vehicle: Energy management and speed optimization,” in *IEEE Intelligent Vehicles Symposium, Proceedings*, 2013, pp. 1434–1439.

[42] G. Mahler and A. Vahidi, “An Optimal Velocity-Planning Scheme for Vehicle Energy Efficiency Through Probabilistic Prediction of Traffic-Signal Timing,” *IEEE Trans. Intell. Transp. Syst.*, vol. 15, no. 6, pp. 2516 – 2523, 2014.

[43] H. Rakha and R. K. Kamalanathsharma, “Eco-driving at signalized intersections using V2I communication,” in *Proceedings of the 2011 14th International IEEE Conference on Intelligent Transportation Systems (ITSC)*, 2011, pp. 341–346.

[44] M. Muñoz-organero and V. C. Magaña, “Validating the Impact on Reducing Fuel Consumption by Using an EcoDriving Assistant Based on Traffic Sign Detection and Optimal Deceleration Patterns,” *IEEE Trans. Intell. Transp. Syst.*, vol. 14, no. 2, pp. 1023–1028, 2013.

[45] F. Jiménez, J. L. López-Covarrubias, W. Cabrera, and F. Aparicio, “Real-time speed profile calculation for fuel saving considering unforeseen situations and travel time,” *Intell. Transp. Syst. IET*, vol. 7, no. 1, pp. 10–19, Mar. 2013.

[46] C. Vagg, C. J. Brace, D. Hari, S. Akehurst, J. Poxon, and L. Ash, “Development and Field Trial of a Driver Assistance System to Encourage Eco-Driving in Light Commercial Vehicle Fleets,” *IEEE Trans. Intell. Transp. Syst.*, vol. 14, no. 2, pp. 796–805, Jun. 2013.

[47] M. Wang, S. Hoogendoorn, W. Daamen, and B. van Arem, “Potential impacts of ecological adaptive cruise control systems on traffic and environment,” *IET Intell. Transp. Syst.*, vol. 8, no. 2, pp. 77–86, Mar. 2014.

[48] T. van Keulen, B. de Jager, a. Serrarens, and M. Steinbuch, “Optimal Energy Management in Hybrid Electric Trucks Using Route Information,” *Oil Gas Sci. Technol. – Rev. l’Institut Français du Pétrole*, vol. 65, no. 1, pp. 103–113, Aug. 2009.

[49] T. van Keulen, B. de Jager, D. Foster, and M. Steinbuch, “Velocity Trajectory optimization in Hybrid Electric trucks,” *Proc. 2010 Am. Control Conf.*, pp. 5074–5079, Jun. 2010.

[50] M. Vajedi, A. Taghavipour, and N. L. Azad, “Traction Motor Power Ratio and Speed Trajectory Optimization for Power Split PHEVs Using Route Information,” in *Proceedings of the ASME 2012 International Mechanical Engineering Congress and Exposition*, 2012, vol. 11, pp. 1–8.

[51] F. Mensing, R. Trigui, and E. Bideaux, “Vehicle trajectory optimization for hybrid vehicles taking into account battery state-of-charge,” in *Proceedings of the 2012 IEEE Vehicle Power and Propulsion Conference (VPPC)*, 2012, pp. 950–955.

[52] G. De Nunzio, C. Canudas de Wit, P. Moulin, and D. Di Domenico, “Eco-driving in urban traffic networks using traffic signal information,” in *Proceedings of the 2013 IEEE 52nd Annual Conference on Decision and Control (CDC)*, 2013, pp. 892–898.

[53] G. De De Nunzio, C. C. De Wit, and P. Moulin, “Urban Traffic Eco-driving : A Macroscopic Steady-State Analysis,” in *Proceedings of the European Control Conference*, 2014, pp. 2581–2587.

[54] A. Freuer and H.-C. Reuss, “Consumption Optimization in Battery Electric Vehicles by Autonomous Cruise Control using Predictive Route Data and a Radar System,” *SAE Tech. Pap. 2013-01-0984*, pp. 304–313, Apr. 2013.

[55] W. Dib, A. Chasse, P. Moulin, A. Sciarretta, and G. Corde, “Optimal energy management for an electric vehicle in eco-driving applications,” *Control Eng. Pract.*, vol. 29, pp. 299–307, Aug. 2014.

[56] J. Rios-Torres, P. Sauras-Perez, R. Alfaro, J. Taiber, and P. Pisu, “Eco-Driving System for Energy Efficient Driving of an Electric Bus,” *SAE Int. J. Passeng. Cars – Electron. Electr. Syst.*, 2015.

[57] L. Li, D. Wen, and D. Yao, “A Survey of Traffic Control With Vehicular Communications,” *IEEE Trans. Intell. Transp. Syst.*, vol. 15, no. 1, pp. 425–432, 2014.

[58] C. P. Pappis and E. H. Mamdani, “A Fuzzy Logic Controller for a Trafc Junction,” *IEEE Trans. Syst. Man Cybern.*, vol. 7, no. 10, p. 707,717, 1977.

[59] U.S. Department of Transportation, “National Strategy to Reduce Congestion on America’s Transportation Network,” 2006.

[60] K. Dresner and P. Stone, “A Multiagent Approach to Autonomous Intersection Management,” *J. Artif. Intell. Res.*, vol. 31, pp. 591–653, 2008.

[61] K. Dresner and P. Stone, “Multiagent traffic management: a reservation-based intersection control mechanism,” in *Proceedings of the Third International Joint Conference on Autonomous Agents and Multiagents Systems*, 2004, pp. 530–537.

[62] S. Huang, A. W. Sadek, and Y. Zhao, “Assessing the Mobility and Environmental Benefits of Reservation-Based Intelligent Intersections Using an Integrated Simulator,” *IEEE Trans. Intell. Transp. Syst.*, vol. 13, no. 3, p. 1201,1214, 2012.

[63] T.-C. Au and P. Stone, “Motion Planning Algorithms for Autonomous Intersection Management,” in *AAAI 2010 Workshop on Bridging the Gap Between Task and Motion Planning (BTAMP)*, 2010.

[64] A. de La Fortelle, “Analysis of reservation algorithms for cooperative planning at intersections,” *13th Int. IEEE Conf. Intell. Transp. Syst.*, pp. 445–449, Sep. 2010.

[65] K. Zhang, A. D. La Fortelle, D. Zhang, and X. Wu, “Analysis and Modeled Design of One State-Driven Autonomous Passing-Through Algorithm for Driverless Vehicles at Intersections,” *2013 IEEE 16th Int. Conf. Comput. Sci. Eng.*, pp. 751–757, Dec. 2013.

[66] C. Wuthishuwong and A. Traechtler, “Coordination of Multiple Autonomous Intersections by Using Local Neighborhood Information,” in *2013 International Conference on Connected Vehicles and Expo*, 2013, pp. 48–53.

[67] Q. Jin, G. Wu, K. Boriboonsomsin, M. Barth, and S. Member, “Platoon - Based Multi - Agent Intersection Management for Connected Vehicle,” *2013 16th Int. IEEE Conf. Intell. Transp. Syst.*, no. Itsc, pp. 1462–1467, 2013.

[68] L. Li and F.-Y. Wang, “Cooperative Driving at Blind Crossings Using Intervehicle Communication,” *IEEE Trans. Veh. Technol.*, vol. 55, no. 6, p. 1712,1724, 2006.

[69] G. Raravi, V. Shingde, K. Ramamritham, and J. Bharadia, “Merge algorithms for intelligent vehicles,” in *Next Generation Design and Verification Methodologies for Distributed Embedded Control Systems*, 2007, pp. 51–65.

[70] F. Yan, M. Dridi, and A. El Moudni, “Autonomous vehicle sequencing algorithm at isolated intersections,” *2009 12th Int. IEEE Conf. Intell. Transp. Syst.*, pp. 1–6, Oct. 2009.

[71] I. H. Zohdy, R. K. Kamalanathsharma, and H. Rakha, “Intersection management for autonomous vehicles using iCACC,” *2012 15th Int. IEEE Conf. Intell. Transp. Syst.*, pp. 1109–1114, Sep. 2012.

[72] Q. Jin, G. Wu, K. Boriboonsomsin, and M. Barth, “Multi-Agent Intersection Management for Connected Vehicles Using an Optimal Scheduling Approach,” *2012 Int. Conf. Connect. Veh. Expo*, pp. 185–190, Dec. 2012.

[73] J. Wu, F. Perronnet, and A. Abbas-Turki, “Cooperative vehicle-actuator system: a sequence-based framework of cooperative intersections management,” *Intelligent Transport Systems, IET*, vol. 8, no. 4. pp. 352–360, 2014.

[74] F. Zhu and S. V. Ukkusuri, “A linear programming formulation for autonomous intersection control within a dynamic traffic assignment and connected vehicle environment,” *Transp. Res. Part C Emerg. Technol.*, Jan. 2015.

[75] J. Wu, F. Yan, and A. Abbas-Turki, “Mathematical proof of effectiveness of platoon-based traffic control at intersections,” *16th Int. IEEE Conf. Intell. Transp. Syst. (ITSC 2013)*, no. Itsc, pp. 720–725, Oct. 2013.

[76] J. Lee and B. Park, “Development and Evaluation of a Cooperative Vehicle Intersection Control Algorithm Under the Connected Vehicles Environment,” *IEEE Trans. Intell. Transp. Syst.*, vol. 13, no. 1, pp. 81–90, 2012.

[77] J. Lee, B. (Brian) Park, K. Malakorn, and J. (Jason) So, “Sustainability assessments of cooperative vehicle intersection control at an urban corridor,” *Transp. Res. Part C Emerg. Technol.*, vol. 32, pp. 193–206, Jul. 2013.

[78] G. R. De Campos, P. Falcone, and J. Sjoberg, “Autonomous Cooperative Driving: a Velocity-Based Negotiation Approach for Intersection Crossing,” in *16th International IEEE Conference on Intelligent Transportation Systems*, 2013, no. Itsc, pp. 1456–1461.

[79] M. a. S. Kamal, J. Imura, a. Ohata, T. Hayakawa, and K. Aihara, “Coordination of automated vehicles at a traffic-lightless intersection,” *16th Int. IEEE Conf. Intell. Transp. Syst. (ITSC 2013)*, no. Itsc, pp. 922–927, Oct. 2013.

[80] M. A. S. Kamal, J. Imura, T. Hayakawa, A. Ohata, and K. Aihara, “A Vehicle-Intersection Coordination Scheme for Smooth Flows of Traffic Without Using Traffic Lights,” *IEEE Trans. Intell. Transp. Syst.*, no. 99, 2014.

[81] M. R. Hafner, D. Cunningham, L. Caminiti, and D. Del Vecchio, “Cooperative Collision Avoidance at Intersections: Algorithms and Experiments,” *Intell. Transp. Syst. IEEE Trans.*, vol. 14, no. 3, pp. 1162–1175, 2013.

[82] A. C. Charalampidis and D. Gillet, “Speed profile optimization for vehicles crossing an intersection under a safety constraint,” in *2014 European Control Conference (ECC)*, 2014, pp. 2894–2901.

[83] I. H. Zohdy and H. Rakha, “Game theory algorithm for intersection-based cooperative adaptive cruise control (CACC) systems,” *2012 15th Int. IEEE Conf. Intell. Transp. Syst.*, pp. 1097–1102, Sep. 2012.

[84] D. Miculescu and S. Karaman, “Polling-Systems-Based Control of High-Performance Provably-Safe Autonomous Intersections,” in *53rd IEEE Conference on Decision and Control*, 2014.

[85] V. Milanés, J. Pérez, and E. Onieva, “Controller for Urban Intersections Based on Wireless Communications and Fuzzy Logic,” *IEEE Trans. Intell. Transp. Syst.*, vol. 11, no. 1, pp. 243–248, 2010.

[86] V. Milanés, J. Alonso, L. Bouraoui, and J. Ploeg, “Cooperative Maneuvering in Close Environments Among Cybercars and Dual-Mode Cars,” *IEEE Trans. Intell. Transp. Syst.*, vol. 12, no. 1, pp. 15–24, 2011.

[87] E. Onieva, V. Milanés, J. Villagrá, J. Pérez, and J. Godoy, “Genetic optimization of a vehicle fuzzy decision system for intersections,” *Expert Syst. Appl.*, vol. 39, no. 18, pp. 13148–13157, Dec. 2012.

[88] M. R. Hafner, D. Cunningham, L. Caminiti, and D. Del Vecchio, “Automated Vehicle-to-Vehicle Collision Avoidance at Intersections,” in *18th ITS World Congress*, 2011.

[89] A. Colombo and D. Del Vecchio, “Least Restrictive Supervisors for Intersection Collision Avoidance: A Scheduling Approach,” *IEEE Trans. Automat. Contr.*, vol. Provisiona, 2014.

[90] X. Qian, J. Gregoire, F. Moutarde, and A. de La Fortelle, “Priority-based coordination of autonomous and legacy vehicles at intersection,” in *IEEE 17th International Conference on Intelligent Transportation Systems*, 2014, pp. 1166–1171.

[91] J. Alonso, V. Milanés, J. Pérez, E. Onieva, C. González, and T. de Pedro, “Autonomous vehicle control systems for safe crossroads,” *Transp. Res. Part C Emerg. Technol.*, vol. 19, no. 6, pp. 1095–1110, Dec. 2011.

[92] W. Wu, J. Zhang, A. Luo, and J. Cao, “Distributed Mutual Exclusion Algorithms for Intersection Traffic Control,” *IEEE Trans. Parallel Distrib. Syst.*, vol. 26, no. 1, pp. 65–74, 2015.

[93] J. Khoury and J. Khoury, “Passive, decentralized, and fully autonomous intersection access control,” in *2014 IEEE 17th International Conference on Intelligent Transportation Systems*, 2014, pp. 3028 –3033.

[94] F. Tedesco, D. M. Raimondo, A. Casavola, and J. Lygeros, “Distributed collision avoidance for interacting vehicles : a command governor approach,” in *IFAC Proceedings Volumes (IFAC-PapersOnline) (2010)*, 2010, pp. 293–298.

[95] G. R. Campos, P. Falcone, H. Wymeersch, R. Hult, and J. Sjoberg, “Cooperative receding horizon conflict resolution at traffic intersections,” in *53rd IEEE Conference on Decision and Control*, 2014, pp. 2932–2937.

[96] L. Makarem and D. Gillet, “Fluent coordination of autonomous vehicles at intersections,” *2012 IEEE Int. Conf. Syst. Man, Cybern.*, pp. 2557–2562, Oct. 2012.

[97] L. Makarem, D. Gillet, and S. Member, “Model predictive coordination of autonomous vehicles crossing intersections,” in *2013 16th International IEEE Conference on Intelligent Transportation Systems*, 2013, no. Itsc, pp. 1799–1804.

[98] K.-D. Kim and P. R. Kumar, “An MPC-Based Approach to Provable System-Wide Safety and Liveness of Autonomous Ground Traffic,” *IEEE Trans. Automat. Contr.*, vol. 59, no. 12, pp. 3341–3356, 2014.

[99] X. Qian, J. Gregoire, A. De La Fortelle, and F. Moutarde, “Decentralized model predictive control for smooth coordination of automated vehicles at intersection,” in *European Control Conference*, 2015.

[100] M. Tlig, O. Buffet, and O. Simonin, “Decentralized traffic management: A synchronization-based intersection control,” *2014 Int. Conf. Adv. Logist. Transp.*, pp. 109–114, May 2014.

[101] M. Tlig, O. Buffet, and O. Simonin, “Stop-Free Strategies for Traffic Networks : Decentralized On-line Optimization,” in *21th European Conference on Artificial Intelligence*, 2014.

[102] P. Sharer, A. Rousseau, D. Karbowski, and S. Pagerit, “Plug-in Hybrid Electric Vehicle Control Strategy: Comparison between EV and Charge-Depleting Options,” *SAE Tech. Pap. 2008-01-0460*, 2008.

[103] L. Guzzella, *Introduction to Modeling and Control of Internal Combustion Engine Systems*. Springer, Dordrecht, 2009.

[104] J. Liu and H. Peng, “Modeling and Control of a Power-Split Hybrid Vehicle,” *IEEE Trans. Control Syst. Technol.*, vol. 16, no. 6, p. 1242,1251, 2008.

[105] “Google Transit.” [Online]. Available: https://developers.google.com/transit/overview.

[106] R. Margiotta and D. Snyder, “An agency guide on how to establish localized congestion mitigation programs,” 2011.

[107] M. A. S. Kamal, M. Mukai, J. Murata, and T. Kawabe, “Model Predictive Control of Vehicles on Urban Roads for Improved Fuel Economy,” *IEEE Trans. Control Syst. Technol.*, vol. 21, no. 3, pp. 831–841, 2013.